

A MATHEMATICAL MODEL FOR TEMPERATURE AND HEAT LOSS CHARACTERISTICS
OF UNDERFLOOR ELECTRICAL RESISTANCE HEATING AND STORAGE SYSTEM

by

TRUNG QUANG HOANG

B.S., Kansas State University, 1983

A MASTER'S THESIS

submitted in partial fulfillment of the
requirements for the degree

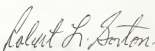
MASTER OF SCIENCE

Department of Mechanical Engineering

KANSAS STATE UNIVERSITY
Manhattan, Kansas

1985

Approved by:



Major Professor

LD
2668
T4
1985
H62
c.2

021169 20211A

TABLE OF CONTENTS

LIST OF TABLES	iii
LIST OF FIGURES	iv
Chapter	
I. INTRODUCTION	1
II. DESCRIPTION	2
Building Description	2
Model Description	7
III. COMPUTER MODEL DEVELOPMENT	10
Literature Review	10
Finite Difference Model	14
Two Cases of Program Model	27
Energy Balance of System	29
IV. VERIFICATION OF COMPUTER PROGRAM	32
Early Fall Comparison	32
Late Winter Comparison	33
Tabulation of Heat Loss Comparison	34
V. COMPUTED RESULTS AND DISCUSSION	45
Effect of Soil Property Values	45
Effect of Building Thermal Transmittance	50
Effect of Edge Insulation	55
Effect of Berm Case	58
Effect of Heat Input Intensity	61
Effect of On-Off Operating Schedule	65
Effect of Climate Condition	67
VI. SUMMARY AND CONCLUSION	73
LIST OF REFERENCES	75
APPENDIX A LIST OF SYMBOLS	77
APPENDIX B LIST OF AUXILIARY EXPRESSIONS	83
APPENDIX C COMPUTER PROGRAM	98
APPENDIX D COMPUTER SAMPLE RESULTS FOR BERM AND NO-BERM	113

LIST OF TABLES

Table	Page
1. Parameters of Soil and Air Temperature Expressions	12
2. Material Properties	12
3. Heat Configuration of Model and Olathe Building	43
4. Building Temperatures and Heat Flows for Variant Thermal Transmittance and Air Temperature	54
5. Values of Edge Loss at Different Edge Insulation Thickness . . .	57
6. Pattern of Heat Flows and Temperature Distributions of the Embankment and Level Buildings	60
7. Heat Flow and Temperature Characteristics at Different Rates of Heat Input	66
8. Temperature Pattern at Variant Ambient Air Temperatures	71

LIST OF FIGURES

Figure	Page
1. Building Cross Section and Heat Transfer Direction	4
2. Heating Mat Layout and Pole Locations Beneath Building	5
3. Thermocouple Location Configuration at KP&L's Warehouse	6
4. Heat Transfer Pattern and Portions	8
5. Slab Below-Grade Configuration of Expressions	17
6. Slab On-Grade Configuration of Expressions	17
7. Building Temperature and Heat Transfer Coefficient for Model . .	19
8. Boundary Condition Assumptions Used in the Model of a Level Building	19
9. Grid Division and Temperature Node Designation for a Level Building	21
10. Grid Division and Temperature Node Designation for a Berm Building	23
11. Heat Flow Configuration of Berm Case	30
12. Heat Flow Configuration of No-Berm Case	30
13. Computed and Measured Temperatures at End of 16 Hour Operation in Early Fall	33
14. Computed and Measured Temperatures at End of 8 Hour Nonoperation in Early Fall	34
15. Temperature Comparison on January 27, 1985 at the End of 16 Hour On-Operating (8:00 a.m.)	39
16. Temperature Comparison on January 27, 1985 at the End of 8 Hour Nonoperating (4:00 p.m.)	40
17. Monthly Average Air and Soil Temperatures of Manhattan, KS . .	36
18. Average Air Temperature Pattern of Manhattan, KS for December 1-15, 1984	38
19. Heat Flow Paths for Variable Soil/Stone Property	47

LIST OF FIGURES

(Continued)

Figure	Page
20. Heat Flow Paths for Variable Concrete Property	48
21. Heat Flow Paths for Variable Sand Property	49
22. Heat Flow Pattern of Thermal Transmittance and Air Temperature Variances	51
23. Heat Flow Pattern of Varying Edge Insulation Thickness and Ambient Temperatures	56
24. Heat Flow Behavior for Heat Input Intensity at Different Thermal Transmittance	63
25. Temperature Distribution of Variant Heat Input at Different Thermal Transmittance	64
26. Heat Flow Pattern of Climate Condition	68
27. Hourly Temperature Pattern with a Step Change of Ambient Air Temperature	70
28. Temperature Configuration for Measured Heat Flow Estimate . . .	95

CHAPTER I

INTRODUCTION

Most energy consuming systems are built to respond to an instantaneous demand for energy. The energy demand is either determined by human operator turning a system "on" or by control system sensing need for energy and initiating steps to satisfy that need. Either way of operation requires that the utility supplying energy is able to meet the total instantaneous demand of all consumers connected to the system. However, the cycles of human and industrial and commercial activity during a 24-hour period are such that "peaks" and "valleys" of energy demand occur. Consequently, the utility must have sufficient capacity to meet the peaks, while some fraction of the generating equipment will be on standby status during the remainder of the time. If any of the consumers energy demands can be shifted off the peak hours, the utility would need a lesser maximum capacity at the peak and the equipment would be better utilized for the remainder of the time.

The problem of peak-valley energy demand occurrence has been long recognized. Utilities and others have sought effective storage devices. The storage device uses surplus capacity to generate energy for storage and subsequent use during peak hours. Examples are storage cells and pumped storage systems of use by electric utilities. Another means of control of the peak is to shift some uses to off-peak times. Some utilities accomplish this by means of "demand charges" and/or by time-of-day pricing -- lower rates for off-peak use. Provision of thermal energy for building heating is a service which could be switched to off-peak by using effective storage

system for the thermal energy. Systems are in use or under study which convert electrical energy into thermal energy for storage in water, high temperature ceramic bricks, and phase-change materials.

An apparently cost-effective system for thermal energy storage is in the earth itself, or, in a bed of sand located on the earth surface below the floor of a one-story building. Such a system consists of high resistance cables which are buried in a sand bed. Electrical energy is converted in the resistance cables into thermal energy during off-peak hours and the sand serves as the thermal storage medium. The system is designed to allow natural processes of heat conduction to transfer energy to the floor surface then to the building when heating is in demand during occupied hours. Numerous of these systems are reported operating in the USA (1).

The purpose of the work described here is to provide a detailed study of such a system. The study consists of two parts:

1 - Collection of energy consumption and temperature data for an existing system.

2 - Development of a heat transfer calculation model and comparison of its results (temperatures and energy use patterns) to the actual system data.

The ultimate purpose is to use the results of this study as basis for development of a guide for designers of such systems in areas similar to Kansas in climate and soil properties.

The existing system which was studied is one installed in a warehouse area at Kansas Power and Light Service Center in Olathe, KS. The system was installed (47 kw) in 1981 when the center was built.

The computer program is a two-dimensional, transient, finite difference representation of storage bed, building, and surrounding earth both adjacent to and under the building floor.

CHAPTER II

DESCRIPTION

Building Description

The Kansas Power and Light Service Center's (KP&L's) warehouse is an 80' X 75' X 17' metal building with its roof insulated to R-30, wall insulated to R-13, and footing insulated to R-6. The south wall is adjacent to the independently heated office building. The north wall is concrete to the 7.5 foot height with earth berm. The west wall is sheltered by a roof covered truck loading dock. The east wall is exposed to outside air; and its floor is at grade level. A typical building cross section is shown in Figure 1.

Location of heating mats is shown on the plan view in Figure 2. The heating mats are controlled in two zones by separate thermostats. The thermostat located inside the building activates the heating mat during the hours 4:00 p.m. to 8:00 a.m. whenever the thermostat sensor temperature drops below 65°F.

The heating mats are at 1.5 feet below the floor surface. A 36" X 3' single mat is rated at 1965 watts (208 volts and 9.45 amperes). The total for all heating mats in the building is 47 kw.

For purposes of the experiment, KP&L metered electrical input to heater mats at 1/2 hour intervals, and provided data monthly showing time and kw-demand.

Temperature information was gathered from thermocouples located as shown in Figure 3. For below-grade measurement, the Cu-Cu thermocouples are mounted on 12" oak pole. The pole was placed inside a 4" bored hole. This thermo-

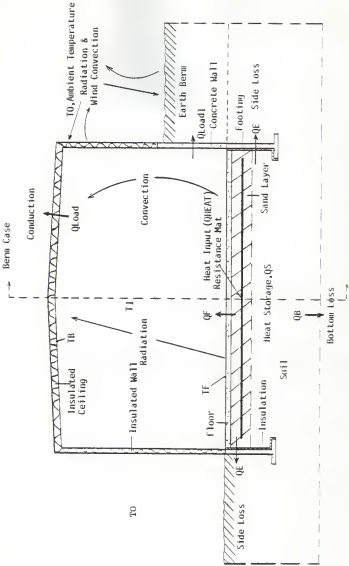


figure 1. Building Cross Section and Heat Transfer Direction.

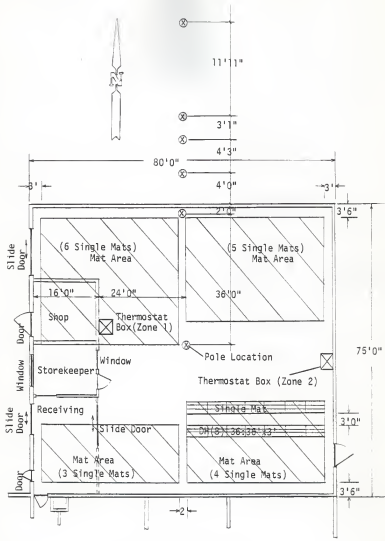


Figure 2. Heating Mat Layout and Pole Locations Beneath Building.

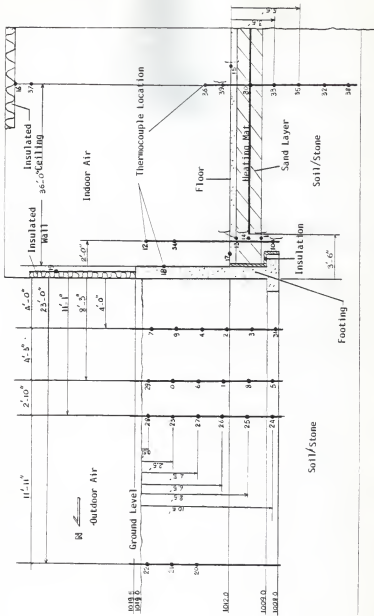


Figure 3. Interocular Lateralization at KPL's Metaposition.

couple design was checked against a different design using a spring loaded mechanism which insured contact with the side of bore hole. The preliminary tests showed no difference in temperatures between the two methods.

There are six poles and six bored holes. Two are inside building, and four others are outside. The outside 4" holes were drilled to 12 foot depth; the pole was inserted into the bored hole and the hole was filled with dirt from the original hole boring. The two inside 4" holes were bored through floor to 10 and 4 foot depth. The pole was inserted and the hole was back-filled with sand. The 10 foot thermocouple pole was located at the center of the building. The 4 foot thermocouple pole was located 1 foot away from the north foundation wall. The 4 foot bored hole depth was limited by a reinforcement bar encountered in the footing. Other thermocouples were taped to floor, wall, and ceiling surfaces as well as suspended in the building air at the locations shown in Figure 3.

All thermocouples were brought to the 40 channel data logger (Monitor Labs Inc., Model 9350) located on the balcony above the shop and storekeeper office area. The logger printer paper was changed by KP&L personnel who also monitored operation of data collection system. Additionally, after initial installation of equipment, several trips were made to the site to check operation and calibration of the equipment.

Model Description

The heat balance model is shown in Figure 4. Electrical energy supplied to the resistance mat is converted into thermal energy, QHeat. The thermal energy is divided into four portions. The first portion, heat gain, QF, is useful heat supplied to building by convection and radiation from the floor surface. The second portion is heat storage, QS, in the sand bed. The other two portions, considered heat losses, are QE and QB conducted through founda-

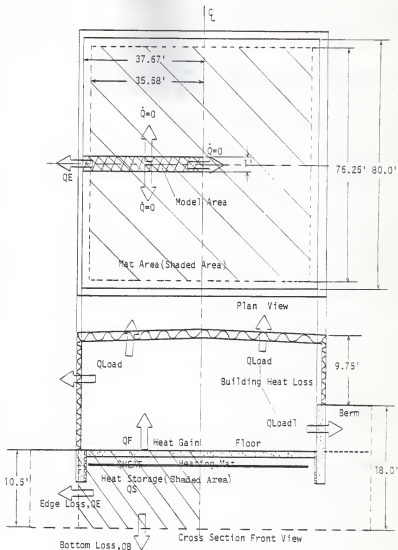


Figure 4. Heat Transfer Pattern and Portions.

tion wall and the earth, respectively. The temperature pattern in a two-dimensional grid is required to calculate the heat flows.

The useful heat (QF) is supplied to offset the heating load of building and serves to maintain the desired building air temperature. The heating load is equal to building heat loss due to heat transmission through building walls and ceiling. Ventilation and infiltration are neglected in the model.

The energy for thermal storage is accumulated in the sand bed when the heating system is on during the off-peak time. This heat resource acts as the heat supply for all heat gains and losses (QF , QB , and QE) when the heating system is turned off during occupied hours.

The heat losses are the heat conducted through the foundation (edge) horizontally and through the bottom (earth) underneath sand bed vertically; these are referred to as edge loss and bottom loss, respectively. The edge loss, QE is determined as the heat conduction through a cross-sectional area extending from the floor to the boundary indicated by dotted line in Figure 4. The bottom loss, QB , is determined as the heat conduction through a cross-sectional area extending from the foundation plane to the center line of the building, as also shown in Figure 4. Simple heat balance equations are shown below.

For operation period, (BTU/hr)

$$\text{Heat input} = \text{heat losses} + \text{heat storage}$$

$$Q_{\text{Heat}} = QF + QB + QE + QS$$

For non-operation period, (BTU/hr)

$$\text{Heat storage} = \text{heat losses}$$

$$-QS = QF + QB + QE .$$

CHAPTER III

COMPUTER MODEL DEVELOPMENT

One purpose of this thesis was to develop a mathematical model to be used to predict the transient temperatures and heat loss for the entire building, including the underfloor portion. The model was to be easily changeable to adapt to a parametric study of the building and heating system. A variable time step iteration technique was used to solve the transient two-dimensional heat conduction finite difference equations in an explicit form.

The following discussion of program development consists of four sections. First, the literature is reviewed for material used to determine boundary conditions for the model. An expression for undisturbed soil temperature for use in the bottom and side boundary conditions is discussed. The literature on soil material properties and on climate conditions is reviewed. Also, the existing literature on underground heat loss calculation is reviewed for comparison to the method selected for this study.

Secondly, the detail of the mathematical model and solution of the resulting equations is discussed. The third section explains the two program cases developed: berm and no-berm. Finally, energy balance introduced into the program for heat flow analysis is discussed.

Literature Review

Soil Temperature and Climate

Four boundary conditions are required for solution of the modeling equations. Two of these, the deep-ground temperature below the storage bed and the undisturbed earth temperature in the area adjacent to the building,

are determined from the expression given below. This expression is in common use and has been shown to accurately determine soil temperatures in various geographic locations (2).

$$T(y,t) = T_m - A_s \cdot \exp(-y(\pi/365A)^{1/2}) + \cos(2\pi n/365 - y(\pi/365A)^{1/2} - D)$$

where:

$T(y,t)$: Ground temperature at depth y and time t ($^{\circ}\text{F}$)

T_m : Annual average soil temperature ($^{\circ}\text{F}$)

A_s : Annual earth surface temperature amplitude ($^{\circ}\text{F}$)

\exp : Exponent in "e" base

D : Phase angle of annual cycle (Rad)

y : Depth of the earth from surface soil (ft)

n : Day number of the date in the year (Day, Jan 1 = 1)

A : Soil thermal diffusivity (ft^2/Day)

Additionally, a daily average air temperature can be derived from the undisturbed soil temperature expression. The air temperature is assumed to be close to the soil surface temperature; the parameters of this equation are given by air temperature data.

$$T_a = T_{ma} - A_{sa} \cdot \cos((2\pi n/365) - Da)$$

where:

T_a : Daily average air temperature at day n ($^{\circ}\text{F}$)

T_{ma} : Annual average air temperature ($^{\circ}\text{F}$)

A_{sa} : Annual amplitude of air temperature ($^{\circ}\text{F}$)

n : Day number of the date in the year (Day)

Da : Phase angle of annual cycle (Rad)

Some desired parameters for both expressions above at particular locations are listed in Table 1. These are taken from ASHRAE Transaction, Vol. 71. (2)

TABLE 1
PARAMETERS OF SOIL AND AIR TEMPERATURE EXPRESSIONS

LOCATION	SOIL PARAMETERS				AIR PARAMETERS		
	TM °F	AS °F	A FT ² /DAY	D RAO	TMA °F	ASA °F	DA RAO
Manhattan, KS	55	27	0.624	0.61	54	26	0.61
Burlington, IA	54	26	0.336	0.57	54	26	0.59
Kansas City, KS	54	22	0.624	0.56	--	--	---
Columbus, OH	53	22	---	0.65	53	23	0.60
Salt Lake City, UT	51	21	0.84	0.48	51	23	0.59
Lexington, KY	55	23	0.60	0.60	56	22	0.60

TABLE 2
MATERIAL PROPERTIES*

Materials	T (°F)	Thermal Conductivity K (BTU/FT-HR-°F)	Density d (Lbm/FT ³)	Heat Capacity Cp (BTU/Lbm°F)	Reference
Air	68	0.0146	0.0735	0.2406	(14) p 5.9
Clay	68	0.739	91.0	0.21	(12) p 555
Concrete	68	0.47 - 0.81 (0.75)	119 - 144 (140)	(0.21)	(12) p 555
Insulation - Broad	75	0.028	17	0.19	(14) p 23.15
Blanket & Batt	75	0.0256	2	0.22	(14) p 23.14
Sand	--	1.14 - 1.41 (1.28)	100 - 12.4 (106)	(0.2)	(15) p 231
Soilstone	68	0.94 - 1.20 (1.07)	135 - 144 (140)	(0.17)	(15) p 555
Steel (Mild)	32	26.5	490	0.11	(16) p 593

* Values in parentheses are chosen to use in model.

Soil Properties

For numerical solution of the model equations, thermal properties of sand, sandstone, and concrete are required. These properties consist of thermal conductivity K (BTU/ft-hr-°F), heat capacity C_p (BTU/Lbm-°F), and density d (Lbm/ft³). These properties vary with the percentage of moisture contained in the soil. However, in this study the percentage of moisture is assumed to be constant. The variation in results as a function of properties is discussed later when K -values between the range of minimum and maximum shown in the table are considered (see K -values in Table 2). Additional information on the influence of percentage of moisture is found in the paper by Gerpen and Shapiro (3).

Previous Studies of Soil Heat Transfer

There are many authors who have done work on soil heat transfer associated with slab on/below-grade buildings. Various methods to solve the heat transfer equations have been used. Szydlowski (4) used two-dimensional, transient, heat conduction equations. The solution for Cartesian coordinates was obtained by using an alternating-direction, implicit iteration technique. Shipp, Pfender, and Bligh (5) also used a transient two-dimensional heat conduction model, solving the finite difference equations by means of an iterative procedure in which the grid points of a single column are evaluated simultaneously. Shen and Ramsey (6) used a Fourier-series Boundary Method to solve the heat-conduction equation with a least squares technique. Drucker and Cheng (7) used an electronic analog computer for a one-dimensional heat transfer model. Kusuda and Achenbach (8) used a finite-difference, time-iteration method to solve the three-dimensional transient heat conduction equation. Wang (9) used the finite element approach to analyze a two-dimensional heat conduction problem with the differential equation converted

into an integral equation. Shipp's (5) work found that the transient two-dimensional heat conduction model achieved good accuracy compared to measured data. The finite difference routine required grid spacings smaller than one foot between grid points.

None of the authors above discussed the disadvantage or advantage of the two-dimensional to the three-dimensional representation. Recently, Delsante, Stokes, and Walsh (10) have done work on heat flow into the ground under a building. Their report used non-steady state two-dimensional and three-dimensional representations of heat flow into the ground. They used the two-dimensional solution and showed that it provided an accurate approximation of the three-dimensional non-steady state heat flow solution obtained with the aid of Fourier transforms. Their results were compared to the results of some authors mentioned above. The report indicated two-dimensional results differ approximately 4% from the three-dimensional results.

After careful study and discussion of all the above valuable literature, the model of this report was developed using the two-dimensional transient heat conduction equation. The solution method was by a forward step time-iteration method. The primary motive for these selections was that sufficient accuracy for purposes of this study could be maintained without the excessively expensive computer time required by the three-dimensional model.

Finite Difference Model

The model is developed into the two regions for which the floor surface is the dividing line - upper- and underslab regions. The upperslab region model is developed as a lumped parameter system. The underslab region model is developed as a two-dimensional heat transfer region. Both regions use the time step iteration to solve for temperatures.

Heat Transfer of Upper Slab Region

The concepts of heat convection, radiation, and conduction using transient state are used in the upper slab region to solve for the temperatures. To do this, well established heat transfer expressions are used to obtain radiative and convective coefficients. Then with these coefficients, building temperature expressions can be solved for the next building temperatures.

Coefficient Expressions:

Coefficient parameters consist of radiative and conductive coefficients. The building ceiling area and the wall area are considered as a single surface. The entire building shape is assumed to be a dome shape for calculating the radiative coefficient. Since the assumed surface is convex, the angle factor (F) between the floor and the ceiling wall surface equals unity.

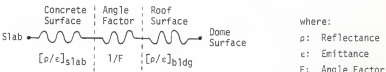
Using an electrical analogy and Kirchoff's law (11), slab radiation (QR) is calculated by:

$$QR = (AF\sigma(TF^4 - TB^4))/R = AF \cdot HR(TF - TB)$$

where:

$$\sigma = \text{Stefan-Boltzmann constant} = 0.1713 \times 10^{-8} \text{ BTU/hr-ft}^2\text{-}^\circ\text{R}^4$$

$$\text{Thermal resistance, } R = [\rho/\epsilon]_{\text{floor}} + 1/F + [\rho/\epsilon]_{\text{building}} + \rho = 1 - \epsilon$$



Also, assuming that dome surface and slab are black bodies, then $\epsilon = 1$. Thus, $R = 1$

From the slab expression,

$$\sigma(TF^4 - TB^4)(TF - TB)/(TF - TB) = HR(TF - TB)$$

where:

$$HR = \sigma(TF^4 - TB^4)/(TF - TB).$$

The convective coefficient expression involves vertical and horizontal surfaces (ASHRAE Fundamental 1981, p. 2.12).

$$\text{Vertical: } H1 = 0.19(TI - TB)^{0.33}$$

$$\text{Horizontal: } H2 = 0.22(TF - TI)^{0.33} \text{ and } H3 = 0.22(TI - TB)^{0.33}$$

A combined radiative-conductive coefficient used for ambient air equals 6.0 BTU/hr-ft²-°F for winter (ASHRAE Fundamental 1981).

Building Temperature Expressions :

The expression for building heat transfer involves the inside building surface temperature (TB) and inside air temperature (TI), along with the inside and outside wall surface temperatures, TWI and TWD. All expressions are based on the transient energy balance concept (Fig. 5, 6, 7). The thermal transmittance of the dome (UB) is the weighted average transmittance value of the ceiling and above-grade wall (Appendix B).

Building temperature is given:

$$TB^* = (\Delta t_1/VB \cdot OB \cdot CPB)[H2 \cdot AR(TI - TB) + H1 \cdot AW(TI - TB) + HR \cdot AF(TF - TB) + UB \cdot AB(TO - TB)] + TB$$

The product of building density ($OB = \text{Lbm/ft}^3$) and heat capacity ($CpB = \text{BTU/Lbm } ^\circ\text{F}$) is determined from a weighted average product ($D \times Cp$) of each material involved with each volume. VB is dome ceiling volume (ft^3) (Appendix B).

Inside air temperature depends on building temperature (TB) and average slab temperature (TF). TF is the average of all slab node temperatures (33 nodes).

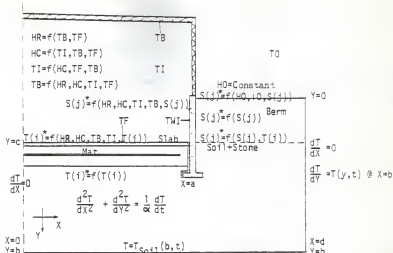


Figure 5. Slab Below-Grade Configuration of Expressions.

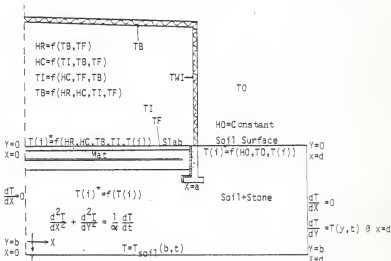


Figure 6. Slab On-Grade Configuration of Expressions.

$$TI^* = (\Delta t)/VAIR \cdot DA \cdot CPA [AR \cdot H2 \cdot (TB - TI) + AW \cdot H1 \cdot (TB - TI) + AF \cdot H2 \cdot (TF - TI)] + TI$$

Inside wall surface temperature (TWI) (figure 7) is:

$$TWI^* = (\Delta t)/VIW \cdot DW \cdot CPW [(KW \cdot AW / WT)(TWO - TWI) + (H1 + HR) \cdot AW \cdot (TI - TWI)] + TWI$$

where:

KW: Wall thermal conductivity (BTU/hr-ft-°F)

WT: Wall thickness (ft)

VIW: Insulated wall volume (ft³)

DW: Wall density (Lbm/ft³)

CPW: Wall heat capacity (BTU/Lbm-°F)

Δt: Time interval for upperslab region (hr)

Outside wall surface temperature (TWO) is:

$$TWO^* = (\Delta t)/VIW \cdot DW \cdot CPW [KW \cdot AW \cdot (TWI - TWO) / WT + AW \cdot HO \cdot (TO - TWO)] + TWO$$

where:

VIW: Wall volume (ft³)

DW: Wall density (Lbm/ft³)

CPW: Wall heat capacity (BTU/Lbm-°F)

WT: Wall thickness (ft)

HO: Combined radiative and wind convective coefficient (BTU/ft²-hr-°F)

Heat Transfer of Underslab Region

The principle used to solve temperature nodes is based on the procedure that Karlekar and Desmond (12) used in their textbook - the principle of conservation energy. This principle is applied to derive a set of finite difference equations in explicit form. A variable time step iteration technique is used to achieve the solutions. The equations are written for a finite number of discrete points within the body and on its surface. The

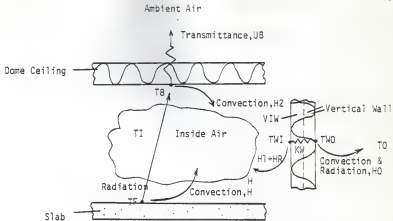


Figure 7. Building Temperature and Heat Transfer Coefficient for Model.

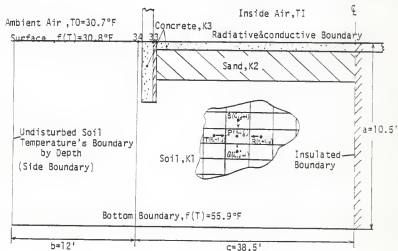


Figure 8. Boundary Condition Assumptions Used in the Model of a Level Building.

equations describe transient, two-dimensional heat transfer. Typically, the process to determine the temperature distributions consists of two steps -- formulation of the modeling equations and execution of the numerical method.

Modeling Equations:

Figure 8 shows the geometry, boundary conditions, and physical properties of the system being modeled. Its geometry is a rectangular shape that is 10.5 feet deep, 50.0 feet long, and 1 foot wide. The rectangular body has four boundaries. The right side vertical boundary is at the centerline of a symmetrical area and is assumed to be an insulated boundary. The left side vertical boundary is 12 feet away from the building edge and is assumed to have the undisturbed soil temperatures increasing from 30.8°F at the surface to 55.9°F at 10.5 feet deep, as mentioned in the previous section.

The top boundary contacting outside and inside air of the building is divided into two portions. First, the outside portion extends from the wall to the undisturbed soil surface temperature node. Combined radiative and forced convective processes relate it to the ambient temperature, T_0 . The inside portion begins with the building edge (node 33), as shown in Figure 8, and continues to the centerline. This portion consists of radiation to the ceiling at temperature, T_B and natural convection to the inside air at temperature, T_I .

The bottom boundary is assumed to be at the undisturbed soil temperature for a depth of 10.5 feet. In this case, the bottom boundary is at a constant temperature of 55.9°F horizontally.

All required properties specified in Figure 8 are listed in Table 2. The nodal temperatures are labeled T with subscript numbers from 1 to 600 and running from right to left as shown in Figure 9 for the case of slab-on-grade. For the case of an earth embankment (berm), a set of temperature equations

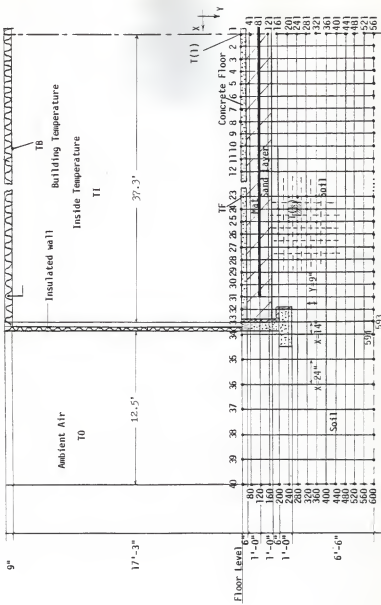


Figure 9. Grid Division and Temperature Node Designation for a Test Building.

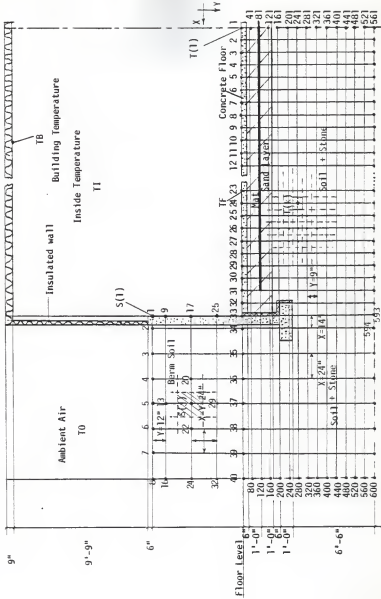
labeled S is used in addition to the "no-berm" equations. S has subscript numbers from 1 to 32 running from right to left as shown in Figure 10. In the berm case, the boundary conditions are different from the no-berm case only on the left side boundary where its boundary condition is given by the undisturbed soil temperature equation at varying depths as mentioned in the previous section. For the berm case, the undisturbed earth temperature difference between 7 foot depth (level with the floor) and 10.5 foot depth is distributed evenly among the 13 nodes.

The area available for heat conduction between two adjacent nodes is the area of the interface between those two nodes. For heat convection, the area is that of the grid surface contacting the air. The area available for heat radiation is the area of the element surface facing the dome ceiling area.

The thermal conductivity and density of materials varies very slightly with the temperature differences for two adjacent nodes. However, the thermal conductivity and density are assumed constant because of the small temperature variations expected. Also, thermal conductivity and the product of density and heat capacity between two adjacent nodes in which there are different materials are evaluated by the weighted average method described in Appendix B. Every heterogeneous grid (e.g. node 33, 41, 121, etc. in Figure 9) requires this treatment.

Temperature Distribution Expressions:

Fourier's Law is applied to the underslab region. The underslab region is simulated as shown in Figure 9 for the no-berm case and in Figure 10 for the berm case. In the no-berm case, the body is divided into a grid pattern which subdivides it into the finite numbers of elements and points called nodes. There is a total of 600 nodes and two different sizes of elements. The size of each underslab element is 9" X 14" where the elements included in the envelope



are from node 1 left to node 33, down to node 593, right to node 561, then up to node 1. The other side is a 9" X 24" element that envelopes the outside building soil region. The shared nodes, 34 down to 594, contain both sizes.

An energy balance is written for each node element. Heat energy is assumed to flow into an internal element $P(i,j)$ (Figure 8) by conduction from the left, from the right, from the top, and from the bottom. The algebraic sum of all four of these contributions must be equal to the change of internal energy of the element $P(i,j)$ under transient conditions.

For a top boundary element, heat energy flows into the element by conduction from the left, from the right, from the bottom, and by radiation and convection from the top. The corner elements at the top boundary are treated specially. Heat energy flows into the insulated boundary element by conduction from the left, the top, and the bottom only. At the right and bottom boundaries, there is no heat energy balance required because the temperature condition is specified.

In the case of many heterogeneous interior nodes involving the above equation, it is kept in the form of integration proceeding for the nodal point P and its nodal coordinates (i,j) . For the general point $P(i,j)$ (see Figure 8 and Appendix B) the equation is:

$$K_{i-1} \cdot \Delta y \cdot 1 \cdot (T_{i-1,j} - T_{i,j}) / \Delta x + K_{i+1} \cdot \Delta y \cdot 1 \cdot (T_{i+1,j} - T_{i,j}) / \Delta x + K_{j-1} \cdot \Delta x \cdot 1 \cdot (T_{i,j-1} - T_{i,j}) / \Delta y + K_{j+1} \cdot \Delta x \cdot 1 \cdot (T_{i,j+1} - T_{i,j}) / \Delta y = \rho \cdot C_p \cdot \Delta x \cdot \Delta y \cdot 1 \cdot (T^*_{i,j} - T_{i,j}) / \Delta t$$

where:

Δx : Element length (ft)

Δy : Element height (ft)

K : Thermal conductivity (BTU/hr-ft-°F)

ρ : Density (Lbm/ft³)

c: Heat capacity (BTU/Lbm-°F)

Δt: Time elapsed from t time to (t + Δt) time (hr)

The superscript (*) indicates future time, t + Δt

At mat nodal points, an internal heat generation \dot{q} (BTU/hr-ft²) is added to the left side of the equation above by the term ($\dot{q} \cdot \Delta x \cdot \Delta z$ where Δz is unity).

For the special elements, one or two terms of the heat conduction equation above may be replaced by radiation terms and/or convection terms. One term of heat flow from the right of the insulated nodal point is eliminated. One term of conductive heat flow from the top is altered by two terms of convection and radiation for slab surface elements. Similarly, one term of heat conduction is replaced by a combined radiative and convective term on soil surface elements.

All general heat transfer equations, except the internal nodal equation already given above, are listed in Appendix B for each particular element type.

A large number of the heat transfer equations -- 600 equations -- are required to determine the temperature distributions. Thus, it becomes impractical to solve this large set of simultaneous algebraic equations by using an implicit formulation (12). For instance, a subroutine SIMQ or MINV for the inverse of the matrix plus GMPRD for the multiplication of the matrix can be used directly on the IBM computers to obtain the solutions. However, the machine storage and time requirements would be excessive. The use of the number of equations may be reduced by using an irregular grid to reduce the number of elements. The grid could be made finer for the nodes that are close to the footing region and made coarser at the nodes away from the footing. However, there is an uncertainty concerning how to regulate the spacing and of

its effect on the accuracy of the temperature distribution. Additionally, a uniform grid was essential in order to exercise and evaluate the program by comparison to Billington's data (13). Consequently, a regular mesh was preferred here.

The solution of unsteady-state problems using the numerical method proceeds from "present" to "future" by using small increments of time. The smaller the time increment used, the greater the resulting accuracy (12). However, if the large increment of time step is used, this will lead to an instability and eventual divergence. To avoid this instability, an implicit formulation may be used, but it involves solving simultaneous equations at each time step (12). Once again, the computer capacity and cost are questioned for solving a 600 X 600 matrix. Consequently, the heat transfer equations were arranged in an explicit formulation, using the iteration method for solution.

Using the explicit form, the heat transfer equation can be rewritten as below, where all future temperatures $T^*(i,j)$ at time $(t + \Delta t)$ are put on the left side of the expression.

$$T^*_{i,j} = (\Delta t / \rho \cdot C_p \cdot \Delta x \cdot \Delta y) \cdot [K_{i-1} \cdot \Delta y \cdot (T_{i-1,j} - T_{i,j}) / \Delta x + K_{i+1} \cdot \Delta y \cdot (T_{i+1,j} - T_{i,j}) / \Delta x + K_{j-1} \cdot \Delta x \cdot (T_{i,j-1} - T_{i,j}) / \Delta y + K_{j+1} \cdot \Delta x \cdot (T_{i,j+1} - T_{i,j}) / \Delta y] + T_{i,j}$$

A similar form to that above was used for each boundary node expression. Altogether, the set of temperature expressions is formed for the underslab region as shown in Appendix C.

The Gauss-Seidel method (12) was used to solve these two sets of expressions, one for the above-slab region and the other for the underslab region. The two regions require different time steps. The variant time step, as well as two independent model cases are discussed below.

Two Cases of Program Model

There is a separate program model developed for each of the two models. The two types of the building structure are only different at the side adjacent to the berm. The first case -- no-berm -- represents a slab built on grade level and having its walls insulated. The second case is the building slab built 7 feet below grade level, where the below-grade wall has 8 inch concrete thickness; this is referred to as the berm building. There is a slight difference in the Gauss-Seidel method applied to these two cases of program models.

No-Berm Program Model

In the temperature distribution expression section, above, expressions were derived for the no-berm case. To begin the solution of temperatures by the iteration method, initial conditions are assumed. The floor node temperature is assumed to be 75°F and the bottom boundary temperature is 55.9°F. The intermediate temperatures underslab only are decreased by linear proportion from 75°F to 55.9°F. The soil node temperatures are assumed to be equal to the undisturbed soil temperatures, related to the depths. The value HR is initially assumed to be 1.04 BTU/ft²-hr-°F, and HC = 0.22, 0.24, 0.19 BTU/ft²-hr-°F for ceiling, floor, and wall respectively. The radiative-convective coefficient is HO = 6 BTU/ft²-hr-°F; building temperature, TB = 72°F; inside air temperature, TI = 73°F; inside wall temperature, TWI = 71.5°F; outside wall temperature, TWO = 31.0°F; outside ambient temperature, TO = 30.7°F (January 6, 1985), and heat input, QHeat = 13.5 BTU/hr-ft². All these assumed values are used in the right side of the underslab temperature expressions, and the new set of the temperature T*'s is obtained. The new slab surface node temperatures then are averaged to get a new TF. Next, the assumed values of TB, TI, HR, HCs, and new TF are fed into the right side of the upperslab

expressions to solve for the new TB, TI, TWI, TWO, HR, and HCs (Figure 6). Finally, these new TB, TI, HR, HCs, and T*'s replace all the originally assumed values for use in the second iteration, and a new set of T*'s is obtained by once again employing the underslab temperature expressions (Appendix B). The iterative process is repeated until 24 iterations are completed per day for 4 days. (See Appendix C.)

Berm Program Model

The Gauss-Seidel method is once again applied to solve the heat transfer equations for the berm case model. This program model added 32 more nodes into the no-berm program mode. This means there are 32 more heat transfer equations which are derived for the temperature distributions of the berm (Figure 10). The function of these added equations is summarized in Figure 5. The temperatures are indicated by symbol S(j).

Internal node equation is given below for $j = 21$ (Figure 10):

$$S^*(j) = (\Delta t / \Delta x \cdot \Delta y \cdot D \cdot C_p) [K_{22} \cdot \Delta x \cdot (S_{22} - S_{21}) / \Delta y + K_{20} \cdot \Delta x \cdot (S_{20} - S_{21}) / \Delta y + K_{13} \cdot \Delta y \cdot (S_{13} - S_{21}) / \Delta x + K_{29} \cdot \Delta y \cdot (S_{29} - S_{21})] + S_{21}$$

The complete set of the berm temperature equations is listed in Appendix C.

The process to achieve the temperature solutions is the same as the process mentioned in the no-berm model previously. Proper determination of time step is essential to satisfy the stability criterion of the solution procedure. This procedure is required due to the stability of temperatures because two regions have a difference of time interval where other factors are fixed in $S(j)$ or $T(k)$'s coefficient term as in the above rearranged equation. The time step is set differently for the upper- and underslab expressions. The time step is set equal to 1.0 hour for underslab expressions. The time step is set equal to 0.2 hours for upperslab expressions. The upperslab

expressions have 5 iterations for each one iteration of the underslab expressions.

Energy Balance of System

Once the temperature distribution of the upper- and underslab is obtained, the heat flow rate can be calculated at each location. The heat loss equations are the same for both the berm and no-berm models except that a wall heat loss (Q_{Load1}) is required additionally for the heat load of berm case. For the underslab region:

(See Figures 11 and 12.)

$$\text{Heat input} = \text{Heat output} + \text{Storage}$$

$$Q_{Heat} = QE + QB + QF + QS$$

For upperslab region:

$$\text{Heat gain through slab} = \text{Heat loss to building} + \text{Storage}$$

$$QF = Q_{Load} + Q_{Load1} + \text{Storage}$$

$$Q_{Load1} = 0 \text{ for no-berm case.}$$

Because of the slight change of the temperatures and the relatively small thermal capacitance, the changes of internal energy are neglected for the inside air temperature node (TI) and for the building temperature node (TB).

A constant heat input ($Q_{Heat} = 13.5 \text{ BTU}/\text{ft}^2\text{-hr}$) is supplied to the mat nodes for the 16 hours from 4:00p.m. to 8:00a.m. of the next day. The system is off ($Q_{Heat} = 0$) for the remaining time of the day.

The amount of heat flow (QF) is the heat gain by the building for heating purposes. This heat gain (QF) is determined as the sum of radiation and convection heat transfers from node 1 to node 33. Heat storage (QS) serves as the heat source supplying heat (QF) during the off-period. Similarly, the edge loss (QE) and soil loss (QB) are the total of all the conduction heat transfer from node 33 to node 553 and from node 521 to 553, respectively. The

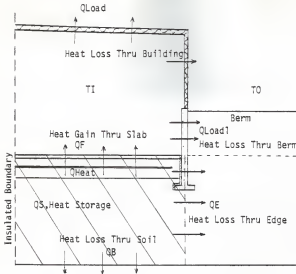


Figure 11. Heat Flow Configuration of Berm Case.

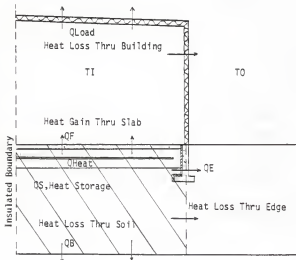


Figure 12. Heat Flow Configuration of No-Berm Case.

heat storage term (Q_S) is the sum of the individual storage amounts for the nodes inside the shaded areas. The heat loss (Q_{Load}) of the building is calculated from the product of average overall building transmittance and the difference between outside and inside temperatures. The heat loss through berm (Q_{Load1}) is a part of Q_{Load} and is calculated separately.

CHAPTER IV

VERIFICATION OF COMPUTER PROGRAM

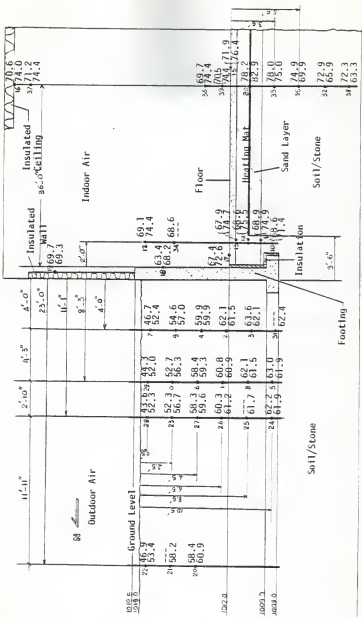
The computer model calculated results for temperatures and heat flows used to compare with the measured results are presented in this chapter. A comparison is presented for two design days for the model and measured data. An early fall day in November and a late winter day in January are chosen. The computed and measured temperatures are presented in Figures 13, 14, 15, and 16. The computed and measured heat flows are shown in Table 3.

Early Fall Comparison

The design day used for both computed and measured results is November 12, 1984. The ambient air temperatures at the site were recorded as 55°F (12.7 °C) maximum, and 36°F (2.2°C) minimum. A temperature of 45°F (7.2°C) was recorded at 7:00 p.m. the same day. The rest of measured temperatures are shown in Figure 13 at the end of a 16-hour operating period (at 8:00 a.m.), and in Figure 14 at the end of 8 hours of nonoperation (at 4:00 p.m.). A constant heat input of 13.5 Btu/hr ft² is used while the existing system operated.

The calculated results are also presented in Figures 13 and 14 for same hour and day. Both computed and measured heat flows are listed in Table 3 and identified by the subtitle of early fall. The same heat input (13.5 Btu/hr ft²) was used in the calculation, and the ambient air temperature was assumed 49.2°F (9.5°C), constantly for the 24-hour period.

From Figures 13 and 14, the inside air temperature of the building



NOTE

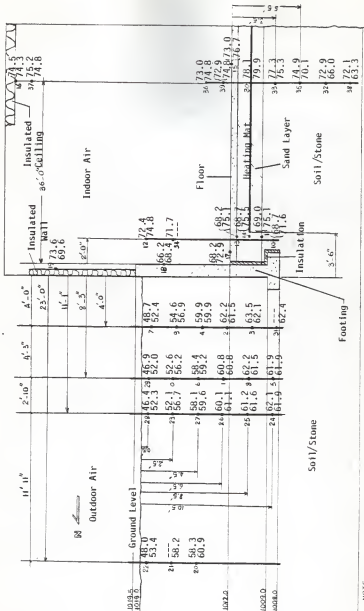
Fig. 8-X: Measured Temperatures

Digitized by srujanika@gmail.com

==: No data or bad data

3

Figure 13. Computed and Measured Temperatures at the End of 16-hour Operation in Early Fall.



HOE

Thermocouple Location - 36 f xx,x: Computed Temperatures

Figure 14. Computed and Measured Temperatures at the End of 8-hour Nonoperation in Early Fall.

(channel 37) is seen to vary 4°F during occupied hours (9 a.m. - 5 p.m.), while the computed temperature varied 0.4°F for the same period. However, both inside air temperatures are almost the same at the end of occupied hours (0.4°F in difference). The building ceiling temperature (channel 16) varied 4.1°F while computed temperature varied 0.3°F during this period. Also, both temperatures are within 0.2°F of each other at the end of period. The floor temperatures (channel 15) behave in the same way as inside air temperatures, but the difference between measured and computed at the end of 8-hour period is 3.7°F. In summary, these computed temperatures in the building are not very sensitive to change while the measured temperatures are more sensitive to variation during 8-hour period. Note here that the building used an electrical back-up heating system suspended under ceiling which was used sometimes (use pattern unknown).

The measured mat-level temperatures (channel 30) are essentially constant during occupied hours (0.1°F change) while the computed values vary somewhat over the same period (3°F change). Calculated and measured temperatures differ only 1.7°F at the end of 8-hour period.

Deeper soil temperatures under slab show a greater difference between measured and computed data. The computed temperatures are lower than the measured temperatures by an average value of 7°F. This is due to the under-building soil being heated by early fall operation of the heating system. The initial condition for computation of soil temperatures is the calculated undisturbed soil temperatures. These undisturbed soil temperatures are much lower than the actual values because an excessive number of iterations would be necessary to provide the necessary "heating" effect. The long time lag for soil heating is illustrated in Figure 17. The deeper soil temperatures' computed and measured values are not much different for the soil adjacent to

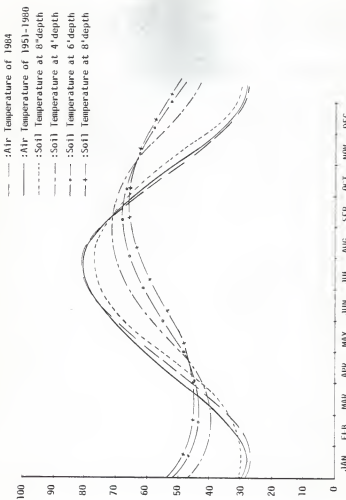


Figure 17. Monthly Average Air and Soil Temperatures of Manhattan, KS.

building wall and foundation where the effect of mat operation has little effect.

The measured and computed temperatures of the soil adjacent to building wall and concrete have a similar pattern except for those temperatures near the surface. The average measured upper soil temperatures vary about 2.5°F during 8-hour period while the computed temperatures are nearly constant. Both temperatures have the same pattern of variation of temperatures after 8 hours below the 2 foot depth. Neither calculated nor measured temperatures are very sensitive to change during this period.

The difference between computed and measured temperatures at the top level around building is affected by the change of ambient air temperature. The computed ambient air temperature was held constant at 49.2°F. Thus, the computed temperatures do not change. The recorded air temperature varies with its minimum value (36°F) occurring at 6:00 a.m. and its maximum value (55°F) occurring at 4:00 p.m. This pattern of variation is indicated in Figure 18 from observation of the air temperature at Manhattan, KS. This natural behavior of air temperature affects the recorded upper soil temperatures as shown in the Figures.

Late Winter Comparison

The design day used for both computed and measured results is January 27, 1984. The ambient air temperature at the site was recorded as 37°F (2.8°C) maximum and 25°F (-3.9°C) minimum. Also, a temperature of 31°F (-0.6°C) was recorded at 7:00 p.m. the same day. The rest of measured temperatures are presented in Figure 15 at the end of a 16-hour operating period (at 8:00 a.m.), and in Figure 16 at the end of an 8-hour nonoperating period (at 4:00 p.m.). A constant heat input of 13.5 Btu/hr ft² is used while the existing system operated.

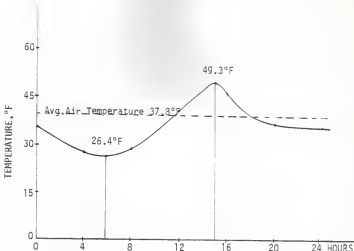
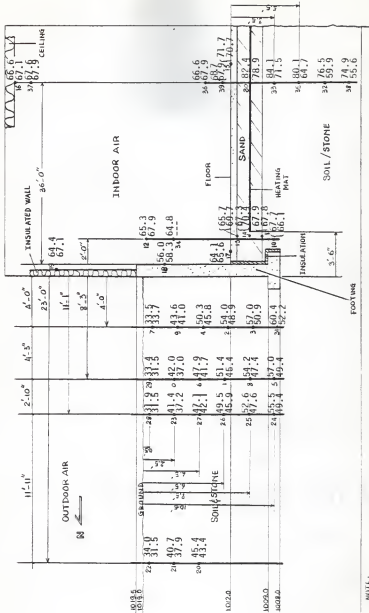


Figure 18. Average Air Temperature Pattern of Manhattan, KS for December 1 - 15, 1984.

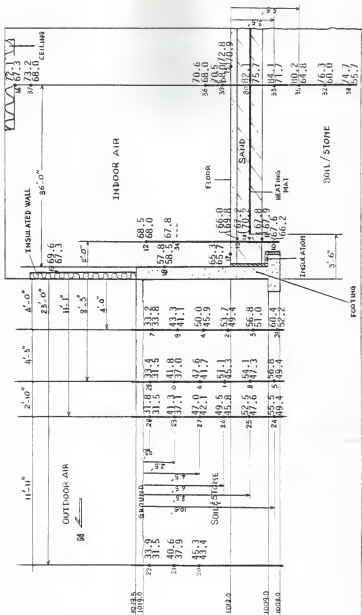
The calculated results are also presented in Figures 15 and 16 for same hour and day. Both calculated and "measured" heat flows are listed in Table 3 and identified by the subtitle of late winter. The same heat input (13.5 Btu/hr ft^2) was used in the calculation. The ambient air temperature was assumed 28.1°F (-2.2°C), constant for the 24-hour period.

From Figures 15 and 16, the inside air temperatures of the building (channel 37) is seen to vary 5.6°F for the measured results compared to 0.1 for computed results over the occupied period (9:00 a.m. - 5:00 p.m.). Replacing the inside air temperature of the building (channel 37) by air temperature at another location (channel 36), the temperature comparison is much closer. The building ceiling temperature (channel 16) varied 5.5°F while computed temperature varied only 0.2°F for the same occupied hours.



NOTE: Channel # --- measured data; - - - computed data; F --- bad data or no data

Figure 15. Temperature Comparison on January 27, 1965 at the end of 16-hour On-operating (8:00 a.m.).



NOTE:

Channel # 36' 0": Measured Data 36' 0": Computed Data

Thermocouple Location

Temperature Comparison on January 27, 1985 at the End of 8-hour Runoperating (4:00 p.m.).

However, the comparison of these computed and measured temperatures of building air (channel 37) and ceiling (channel 16) is nearly identical (Figure 15, 0.5°F and 0.3°F difference for air and ceiling temperatures respectively) at the start of the occupied period.

The floor temperatures (channel 15) behave correspondingly for computed and measured results. The differences of 1°F between calculation and measurement is at 9:00 a.m. and 1.9°F is at 5:00 p.m. However, 1.1°F and 0.2°F changes occurred during an 8-hour period for the computed and measured temperatures. As mentioned in the previous section, the existing building used an electrical back-up heating system whose use pattern was unknown; this interfered with these comparisons of temperatures.

The measured mat-level temperatures (channel 30) are essentially constant during an 8-hour period (0.3 F change) while the computed temperatures vary 3.2 F over the same period. However, the variance of measured and computed temperatures is similar over the same period at channels 33, 35, 32, and 38. But there is noticeable difference between the measured and computed temperatures. Differences of this magnitude also occurred at the locations outside the building but inside the berm below 3 foot depth. As previously explained, these differences between computed and measured temperatures are due to the under-building soil being heated by early operating of the heating system. Additionally, the initial condition for computation of soil temperatures is the calculated undisturbed soil temperatures. The undisturbed soil temperatures are much lower than the actual values because an excessive number of iterations would be essential to provide the necessary "heating" effect. The long time lag for soil heating is illustrated in Figure 17.

The top soil temperatures for computed and measured values are quite similar. For instance, the temperatures at channel 7 varied 0.3°F and 0.1°F

for computed and measured temperatures during an 8-hour period.

In summary, the measured temperatures for locations in the building are more variable than the computed temperatures. But, the computed temperatures show a similar variance to measured temperatures at locations near the sand storage bed (channels 30, 33, and 14). Neither computed nor measured temperatures for the rest of channels vary more than 0.3°F degrees except those mentioned before.

Tabulation of Heat Flow Comparison

A pattern of building heat flows for comparison purposes is presented in Table 3. The Table consists of two sets of heat flow results which are distinguished by designated days of early fall and late winter as mentioned above. Each set contains the results of computed and "measured" heat flows including the percentages of heat distribution (as shown in the Table). The heat flows are designated at the end of operating system period (8:00 a.m.) and at the end of nonoperating system period (4:00 p.m.).

The results of "measured" heat flows are estimated from the temperatures measured at the existing building. The method of estimating building heat flows is detailed in Appendix B. The computed heat flows are from the program output.

The results in Table 3 show that the computed heat flows are more stable than the measured heat flows for both days. For instance, computed heat gain, Q_L , varied 1.8 Btu/hr while measured results varied 19.4 Btu/hr during an 8-hour period for early fall. The measured heat gain at 8:00 a.m. is much higher than that at 4:00 p.m. when the outside air temperature of early morning is much lower than the outside air temperature of late afternoon. Theoretically, the heat gain (Q_F) should be greater than the building loss because Q_F is supposed to be the only heat supply to building. However,

TABLE 3
HEAT CONFIGURATION OF THE MODEL & OAATHE BUILDING

EARLY FALL

	Heat I or R ^a	Heat Gain	Earth Loss	Edge Loss ^b	Heat Storage ^c	Building Loss	Wall+Clg Loss	Beru Loss ^d
E	Q _L BTU/HR	Q _F / BTU/HR	Q _B / BTU/HR	Q _E / BTU/HR	Q _S / BTU/HR	Q/ BTU/HR	Q _{I/Q} / %	Q _{2/Q} / %
Computed	101.2	20.8	51.2	10.5	10.7	2.2	323.1	66.5
Measured	108.1	22.5	60.2	12.5	17 (3.8)	N/A	310.3	64.6
Computed	103.1	62.3	51.7	31.2	10.8	6.5	-160.2	96.8
Measured	89.7	62.4	52.2	36.3	1.8 (3.9)	N/A	-143.7 (-161.4)	0.0

LATE WINTER

	Heat I or R ^a	Heat Gain	Earth Loss	Edge Loss ^b	Heat Storage ^c	Building Loss	Wall+Clg Loss	Beru Loss ^d
E	Q _L BTU/HR	Q _F / BTU/HR	Q _B / BTU/HR	Q _E / BTU/HR	Q _S / BTU/HR	Q/ BTU/HR	Q _{I/Q} / %	Q _{2/Q} / %
Computed	153.8	31.6	85.1	17.5	17.9	3.7	230.9	47.4
Measured	172.2	35.8	80.2	16.7	3.5 (6.6)	N/A	224.4	46.7
Computed	154.9	60.0	85.6	33.1	17.8	6.9	-251.6	97.4
Measured	172.2	66.8	78.2	30.3	3.5 (6.4)	N/A	-257.9 (-229.4)	0.0

^a = I: Input, R:Rejection (negative sign)

^b - The value in parentheses is calculated from the model

^c - The value in parentheses is calculated by weighted average method

^d - Heat loss through 7th grade wall by ASHRAE Fundamental 1981 (p. 26.7) in parentheses (uninsulated) $Q_2 = 1.15 (I_1 - I_0 - A)$ where I_1 : inside air temperature, T_0 : mean air temperature, A : ground surface temperature at altitude (Manhattan: 10° 55' WF, $A = 26^{\circ}\text{F}$, ASHRAE V.71, 1965, p. 63), I_1 : heat loss per per meter = $BTU/FT \cdot 10^{-3}$

measured building load is somewhat higher than the heat gain for early fall day while the computed results correlate well in either early fall or late winter. The earth loss values have similar behavior for both computated and measured values in either early fall or late winter. For instance, computed earth losses, Q_B , are slightly less than measured earth losses (9 Btu/hr and 0.5 Btu/hr at 8:00 a.m. and 4:00 p.m.), for early fall. But, computed earth losses are slightly higher than measured earth losses for late winter.

Due to the assumptions in estimating measured heat flows (Appendix B), the measured edge losses are only comparable to the computed edge losses by their values listed in parentheses underneath measured values. A difference of computed and measured values is smaller for early fall than for late winter; 2.1 Btu/hr compares to 3.1 Btu/hr both for early fall and late winter at 8:00 a.m. and 4:00 p.m., respectively.

Heat storage, Q_S , has a small difference between computed and measured values (about 6 Btu/hr) in late winter; the difference is larger (about 14 Btu/hr) in early fall. However, if the weighted average of the measured values is used, heat storage is different by no more than 6 Btu/hr in general.

Building, wall and ceiling, and berm losses are quite simlar when comparing computed and measured heat losses of late winter. The difference is 6, 3, and 6 Btu/hr of building, wall and ceiling, and berm losses, respectively. This difference is larger when comparing them for early fall.

In summary, the values of computed and measured heat flows are somewhat different due to outside air temperature, back-up heating system, and method of estimate. But, the percentage of heat flow distribution is very simlar for both the calculated and measured results.

CHAPTER V

COMPUTED RESULTS AND DISCUSSION

Many factors influence the behavior of an underfloor electric resistance heating and storage system. In this chapter, several of these factors judged to be important are discussed. The items investigated are: the effect of soil properties, building thermal transmittance, foundation insulation, berm built on building side wall, heat input intensity, on-off schedule for system operation, and climate conditions. Other important factors not discussed here have been studied by others. These include depth of the heating mat, slab thickness, soil properties as influenced by the moisture percentage, and below-grade insulation treatments (3). Additional study has been done on the general heat transfer behavior of a single floor, radiative, slab-heated building; on heat transfer of heat storage area (including response of system to outdoor temperature changes); on downward heat loss into the earth; and on edge heat losses from heat storage area (17).

Effect of Soil Property Values

The material properties of interest include those of the concrete used for slab and foundation, the sand used as heat storage, and the soil/stone layer under the building. The values of these properties were estimated for use in the model (refer to Table 2).

The material properties are thermal conductivity, density, and heat capacity. Thermal conductivity and density values are related to each other.

To study the effect of material properties, the influence of the maximum and minimum values of thermal conductivity and density of each material are

determined. All other properties are held constant for this determination. Values of thermal conductivity and density are estimated and listed in parentheses in Table 2. For example, minimum values of soil/stone properties ($K = 0.94$, $d = 135$, $C_p = 0.17$) are used as variables while sand properties ($K = 1.28$, $d = 106$, $C_p = 0.2$) and concrete properties ($K = 0.75$, $d = 140$, $C_p = 0.21$) are held constant. Replace minimum values by maximum values of soil/stone properties ($K = 1.20$, $d = 144$, $C_p = 0.17$) for the next result. A similar method is applied to the values for sand and for concrete properties.

For these determinations, heat input to resistance mat is 13.5 Btu/hr-ft². Ambient temperature is held at 30.7 °F (-1 °C). The system is modeled to operate 16 hours on, followed by 8 hours off. The results shown in Figures 19, 20, 21 are average values for the 16-hour operating period.

In Figure 19, the influence on heat flow of various soil/stone properties is shown. An increase of thermal conductivity led to an increase of deep earth heat loss and also of edge heat loss. Logically, if more heat is lost to the ground, less heat is stored. The heat storage is seen to decrease sharply when soil/stone thermal conductivity is increased. As the result, the energy available for building heat is slowly decreased due to the resulting drop in slab temperature.

In Figure 20, heat flow is shown as a function of concrete property variation. A change of concrete thermal conductivity has an impact on heat storage (and building heating) and edge heat loss. The building load (heat conducted through slab) and edge heat loss are increased when using higher concrete thermal conductivities. A high concrete thermal conductivity is of benefit to building heating but it leads to higher edge losses (even through a 2" insulation foundation). As a result of this, the heat storage capacity is lessened as concrete conductivities increase. However, a change of

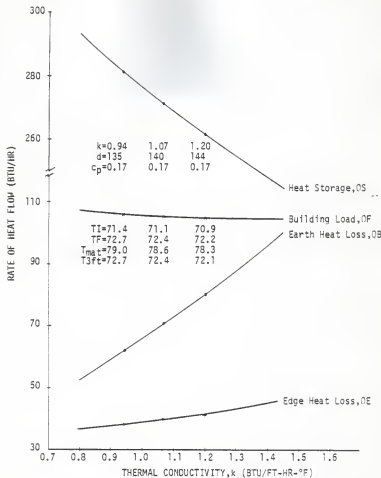


Figure 19. Heat Flow Paths for Variable Soil/Stone Property.

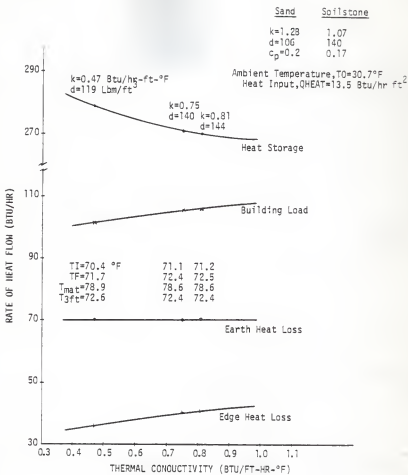


Figure 20. Heat Flow Paths for Variable Concrete Property.

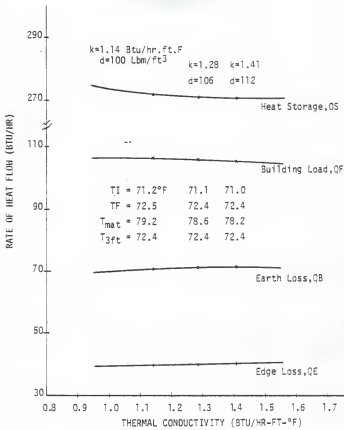


Figure 21. Heat Flow Paths for Variable Sand Property.

concrete conductivity from lowest to highest values resulted in an inside air temperature increase of only about 1 °F.

The results in Figure 21 are for variation of sand properties from minimum to maximum values. A change of sand thermal conductivity and density causes only small variation in heat flows. The greatest variation occurs in the thermal energy storage -- sand bed. An increase of sand thermal conductivity causes a decrease in heat storage, and the earth and edge losses are slightly increased. Consequently, the heat load is almost constant. However, there is an important effect of the sand property on building response. In other words, the number of hours required for building air temperature to respond to a heat input at the mat depends on the value of thermal conductivity used. From computed results, the building air temperature reached its maximum value 6 hours after the maximum mat temperature was reached (for minimum sand property). But, it reached its maximum value with a five hour lag when using the maximum value of the sand property. A careful study of sand thermal diffusivity is used as a guide to decide on a design time lag for the system.

In summary, the variance of earth thermal properties at a building site should be determined carefully. A high value of earth thermal diffusivity would cause significant earth heat loss. As a result, not much heat storage would be available to supply the heating demand during the system's off period.

In addition to foundation insulation, a low thermal diffusivity of the foundation concrete could help to reduce an edge loss.

Effect of Building Thermal Transmittance

Building heat load is supplied by heat radiation and convection to building air from heated slab. This load is transferred to the ambient air

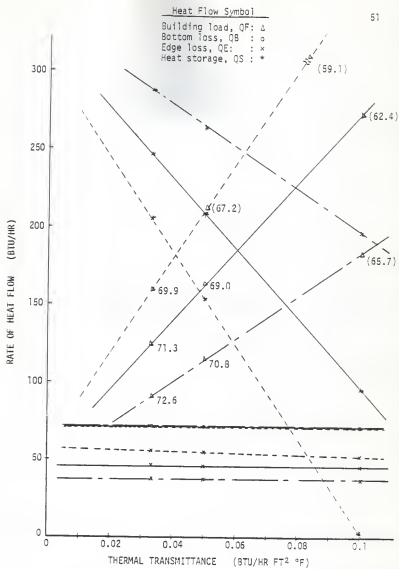


Figure 22. Heat Flow Pattern of Thermal Transmittance and Air Temperature Variances.

heat conduction through the outside building wall and ceiling. To reduce heat loss, the wall and ceiling are built with a layer of insulation inside. This section will study the effect of insulation (in terms of thermal transmittance) which associates with outside temperature and heating load.

To study this effect, building thermal transmittances (U-value, Btu/hr-ft²-°F) are given values 0.1 (R=10 hr·ft²·°F/Btu), 0.05 (R=20), and 0.033 (R=30). Each U-value is studied as a function of ambient air temperatures of -10°F, 10°F, and 30°F. The calculation is begun from conditions established from a previous 24-hour period at 30.7°F. Heat input (QHeat) is held at constant value of 13.5 Btu/ft²·hr.

The computed results as shown in Figure 22 by lines, are indicating heat flows (QF, QB, QE, and QS) and thermal transmittances (U-values). The solid lines refer to heat flows and U-values at an outside air temperature of 10°F. The solid-dotted lines and dotted lines refer to outside air temperatures of 30°F and -10°F, respectively. The values in parentheses indicate an average inside air temperature of building for the 8-hour occupied period.

Figure 22 shows that thermal transmittance of a building has a significant impact on the building heating load and on the underslab thermal storage system. A low U-value (as used for an insulated building) maintains the indoor temperature very well. Using U-value of 0.03 Btu/hr ft² °F, the change of inside air temperature is 2.7°F when outside air temperature drops from 30°F to -10°F. Using a U-value of 0.1 Btu/hr ft² °F, the change is 6.8°F for the same drop of outside air temperature. A big change of building air temperature would require a larger additional amount of heat supply to offset it. However, the larger heat storage needed for building has the disadvantage of preventing the system from responding quickly. As a result, the inside air temperature would maintain a lower value for a long period of

time and would then probably overshoot the desired temperature.

The building load requires a larger amount of heat supply as the U-value increases and air temperature drops. The gradient of the heat flow's curve, as well as for heat storage, is steeper when the air temperature is lower. Heat storage is decreased as the U-value increases and air temperature drops. The dotted line of heat storage indicates that the heat supplied to building during the B-hour period of "off" operation, completely depletes the storage (for a U-value of 0.1).

For the case of 0.05 Btu/hr ft² °F which is a similar value to the actual building of this study, if an outside air temperature drops below 0°F, then heat supply drawn from thermal storage for heating demand would be insufficient during "off" system period. For instance, heat demand for building consisting of QF, QB, and QE requires 333 Btu/hr. Theoretically, heat storage only supplies 306 Btu/hr (table 4) during "off" period. Thus, the heating system requires a higher rate of power in order to maintain the desired inside air temperature when an outside air temperature drops below 0°F.

The case of 0.1 Btu/hr ft² °F for a building allows heat input to barely offset the heat losses from building during "on" period. No net thermal storage is generated if a heat input of 13.5 Btu/hr ft² is used and air temperature is -10°F. In this case, the heating system may be required to operate 24 hours a day, or a 3/4 full capacity may be required to run for 16 hours. Using a constant rate of 13.5 Btu/hr ft² (a half capacity of the existing system), the heating system can only maintain the building air temperature above 65°F if the outdoor air temperature is above 30°F. A higher rate of heat input is required by the system if building is to be maintained at 65°F or above when the outdoor temperature is below 30°F.

TABLE 4
TEMPERATURES AND HEAT FLOWS FOR VARIOUS THERMAL TRANSMITTANCE AND AIR TEMPERATURE

Temperature @ NOON °F		0-0.1 BTU/HR FT² °F			0-0.05 BTU/HR FT² °F			0=0.033 BTU/HR FT² °F					
		Start	-10 °F	10 °F	30 °F	Start	-10 °F	10 °F	30 °F	Start	-10 °F	10 °F	30 °F
LB	TB	64.1	55.6	59.7	63.9	69.5	65.5	67.2	69.8	71.4	68.5	70.2	71.9
LB	TF	68.2	63.6	65.8	68.1	71.9	70.0	71.0	72.2	73.1	71.8	72.7	73.6
LB	TL	65.9	59.1	62.4	65.7	70.5	67.2	69.0	70.8	72.1	69.9	71.3	72.6
LB	Total	77.8	77.4	77.6	77.8	79.1	79.2	79.5	79.7	79.7	80.3	80.4	80.5
LB	T3'	72.3	72.3	72.3	72.3	72.8	73.4	73.4	73.4	73.0	73.7	73.7	73.7
LB	QF	181	360	273	184	103	210	163	114	87	159	124	90
LB	QB	70.5	70.5	70.5	70.5	70.5	70.5	70.5	70.5	70.5	70.5	70.5	70.5
LB	QE	37.5	52	46	37	43	53	46	38	41	55	46	38
LB	QS	196	2	95	194	269	153	208	263	288	206	247	289
LB	Heat Demand	289	482.5	389.5	292	217	333	280	223	199	285	241	199
LB	Heat Resource (Maximum)	392	4	190	388	538	306	416	526	576	412	494	578

The "heat resource" in Table 4 is twice the magnitude of "heat storage (QS)" because QS is an average heat per hour; this is stored during the 16-hour system operation, then the total QS is drawn out during the next 8 hours when system is off. As the results of heat resource listed in Table 4 show, the existing size of heating system is satisfactory for the application of U-values and climate conditions in the Table. A full capacity of the system may be required for use if the air temperature drops below -10°F and $U=0.1 \text{ Btu/hr ft}^2 \text{ }^\circ\text{F}$. Based on Table 4, the "oversize" factor of 1.25 (a national average) can be used for Kansas to design and size an underfloor heating system for 16 on/8 off operation.

A change of U-values and air temperatures in short period does not significantly affect heat loss to the ground. But, it slightly affects the edge loss if the outside air temperature drops to or below -10°F as the results show in Figure 22 and Table 4.

Effect of Edge Insulation

The study of edge heat loss is concerned with the heat conducted through the foundation or below-grade wall. This loss is associated with the outside air temperature. A colder day worsens the edge loss. Most buildings have a layer of insulation put along the inside/outside foundation in an "I" shape or "L" shape. The discussion in this section focuses on the case of insulation along inside foundation in "I" shape.

The effect of edge insulation was studied by determining heat flows as a function of thickness of edge insulation and outside air temperature. The thickness of insulation is varied from 0 to 3 inches. Outside air temperature is set to -10°F, 10°F, and 30°F daily average values.

The heat flows shown in Figure 23 are graphed by hourly average values of computed heat flows for 24-hour period corresponding to each thickness and

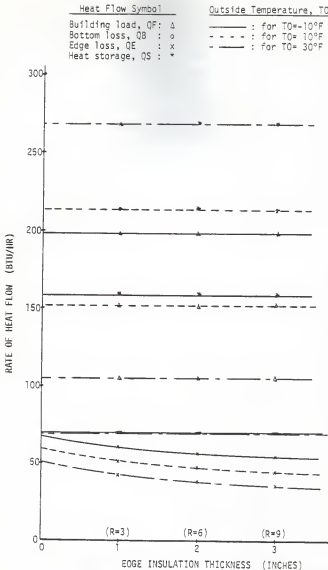


Figure 23. Heat Flow Pattern of Varying Edge Insulation Thickness and Ambient Temperatures.

TABLE 5

VALUES OF EDGE LOSS AT DIFFERENT EDGE INSULATION THICKNESS

T ₀ (°F)	No Insulation	1 Inch	2 Inches	3 Inches
-10	68	60	57	54
10	60	51	48	45
30	51	42	39	36

Edge loss (ΩE) is in BTU/HR T_0 is the daily average ambient air temperatureR is thermal resistance in HR FT²°F/BTU

outside air temperature. However, the heat storages' (QS) input occurs only in the 16-hour period. Thus, average values of heat storage are based on that period. The values of heat flows are computed when the heating system uses a constant heat input of 13.5 Btu/hr ft² for 16 hours then shuts off for 8 hours.

From the results shown in Figure 23, a variation of edge insulation thickness has a direct impact on heat loss (QE). Adding 3 inch thick insulation to an uninsulated foundation would cut the edge loss 30% (values of edge loss shown in Table 5) when outside air temperature is 30°F. However, this percentage is reduced when the ambient air temperature drops. From no insulation to 3 inch insulation added to foundation, the percentage of edge loss is reduced to 25% and 21% when outside air temperatures are 10°F and -10°F respectively.

If 1 inch or 2 inch insulation is added to the uninsulated foundation, then edge loss could be reduced by 17.6% or 23.5% respectively for an outside air temperature of 30°F, by 15% or 20% for outside temperature of 10°F, and by 12% or 16% for outside air temperature of -10°F. With no insulation added to foundation, the edge loss would consume 14% of total heat input for T_O = -10°F, 12% for T_O = 10°F, and 10.6% for T_O = 30°F where T_O is outside air temperature.

Changing edge insulation thickness has little effect on heat storage (QS), heat loss (QB) to the earth, and heating load (QF) to building.

Effect of Berm Case

Buildings may be built in an embankment or underground to reduce heat loss because the soil or berm acts like an insulation. The building of this study was partially built in an embankment. To understand this effect, the computer model was developed to study heat flows and building tempera-

tures for cases both when an embankment does and does not exist. Also, an insulated berm is of interest to the study. The study of this section is based on a daily average air temperature of 30.7°F (-1°C) and a constant heat input of 13.5 Btu/hr ft².

The model is developed for three cases of buildings. The first case assumes that a 7.5' concrete wall is surrounded by soil. No insulation is added to this concrete wall of 8 inch thickness. The second case assumes that a 2" insulation is added to the wall. The final case is the building built on level ground and all its walls are metal pannels with 4 inch insulation.

For each case, the results (heat flows and temperatures) are shown in Table 6. All heat flows are hourly average values in Btu/hr for a 24-hour period, except that heat storage is averaged in the 16-hour period that is the operating time for the system. Qberm listed in the Table is the heat loss through the berm per hour. The values of listed temperatures are at noon for the day of January 6.

Heat flows shown in Table 6 have different behavior for the cases of berm and no-berm buildings except for the heat loss to the earth. An additional heating load of over 8.4% of total heat input is required for the berm case without insulation. Over 47% of heating load is lost through the berm concrete wall. Thus, the heat storage in the berm case absorbed less heat than in the case of no-berm. Because the berm acts like another layer of insulation for the edge loss, the edge loss is reduced in the berm case by over 4% of total heat input for a 7 foot additional soil from the floor. In summary, the heat resource of berm case is only less than the heat resource of no-berm case by 4.3% of total heat input.

If insulation materials of 2 inch thickness are added to the case of the

TABLE 6
PATTERN OF HEAT FLOWS AND TEMPERATURE DISTRIBUTIONS OF THE EMBANKMENT AND LEVEL BUILDINGS

HEAT FLOW BTU/HR		BERM	INSULATED BERM	NO BERM
QF	146	107	105	--
Q Berin (qL0.001)	69	23		
QB	71	71	71	
QE	18	18	39	
QS	251	290	272	
HEAT FLOW BTU/HR				
TB	67.8	71.1	70.3	
TF	70.9	73.4	72.6	
TI	68.5	71.9	71.3	
TEMPERATURE IN AIR @ 16th HR		80.0	79.9	
T3' @ 24th HR		73.5	73.5	

berm building, then the heating load of insulated berm building behaves in the same manner as the no-berm building. Thus, heat storage absorbs 4.3% more of total heat input. Of course, the insulated berm building is better off than the berm building for heating purposes and human comfort when comparing their temperatures.

From temperature results also shown in Table 6, all temperatures of no-berm building have higher values than those of berm case building. In spite of the fact that the heating load of no-berm case is lower than that of berm case, it has the advantage of allowing the inside air temperature to rise -- an increase of 2.8°F degrees. This advantage makes the conditioned air more acceptable for human comfort level (designated 75°F as mentioned in ASHRAE Fundamentals Handbook, 1981, Chapter 8) for no-berm building. Further, the insulated berm building has the greatest advantage for heating purposes. As a result, more heat storage is reserved which brings the slab temperature up as well as the inside air temperature. Consequently, better human comfort can be achieved.

Effect of Heat Input Intensity

The capacity of the simulated heating system is studied for its effect on building temperatures. A set of variable electrical power intensities are used to generate comparisons of the heat flows and temperatures of a building, all with the daily average air temperature of 30.7°F (-1°C) and a fixed operating time for 16 hours of a 24 hour period.

The intensity of heat input varies from 12 to 27 Btu/hr ft² in increments of 5 Btu/hr ft². Two values of thermal transmittance are used, 0.1 and 0.05 Btu/hr ft² °F. The results showing heat flows and building temperatures as a function of intensity of heat input are plotted in Figures 24 and 25. In both figures, the solid lines indicate the results for a building thermal

transmittance of 0.1 Btu/hr ft² °F. The solid-dotted lines refer to the results using a thermal transmittance of 0.05 Btu/hr ft² °F.

An increase of intensity of heat input to the heating system directly affects heat flows and temperatures. The use of higher values of heat input increases the values of heat flows and temperatures.

From Figure 24, there is a strong effect on the heat storage as shown by steeper lines for both values of thermal transmittance. An increased intensity of heat input to the system gives the advantage of greater storage of thermal energy. As a result, there is a greater energy availability for the heating load, but there is an increase in the heat losses to ground and edge. A slight change (20 Btu/Day) of bottom loss occurs when varying heat intensity from 12 to 27 Btu/hr ft², but a larger amount (100 Btu/Day) of heat loss through building edge occurs for this same variance. (U-value is 0.05 Btu/hr ft².) However, building load increases significantly by an amount of 600 Btu/Day for U-value of 0.05 and by 920 Btu/Day for U-value of 0.1 Btu/hr ft² °F. This increase is due to the higher building temperature at the greater intensity.

In Figure 25, the slope of the mat temperature line is larger than the slopes of ceiling, inside air, floor, and 3 foot depth temperature lines. Thus, mat temperatures are more sensitive to varying levels of heat input than other temperatures. Varying U-value only shifts the temperature lines up or down when varying heat input is applied to each U-value.

The change of heat flows and temperatures are related to each other as the variation in intensity of heat input occurs. Higher mat level temperature due to the increasing heat intensity results in a greater heat storage. Greater heat storage and storage bed temperature increases the other heat flows and temperatures. Thus, pattern of temperatures could be useful in

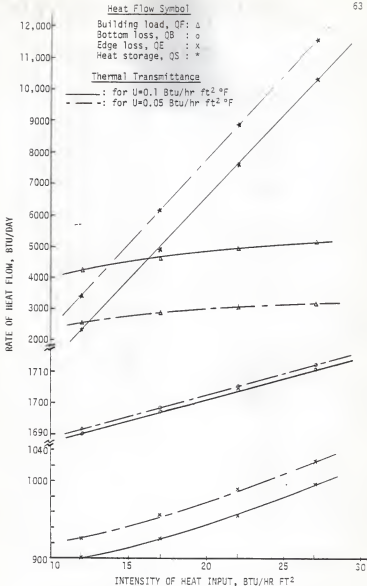


Figure 24. Heat Flow Behavior for Heat Input Intensity at Different Thermal Transmittance.

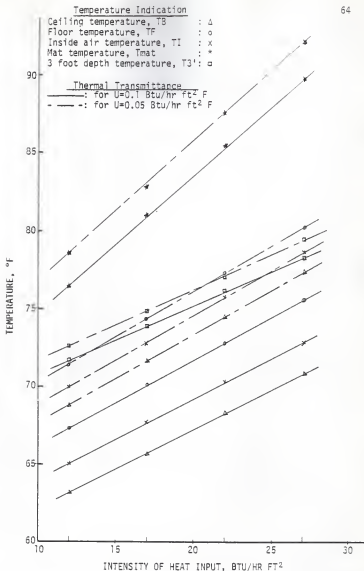


Figure 25. Temperature Distribution of Variant Heat Input at Different Thermal Transmittance.

estimating the intensity of heat input for operating the system effectively.

Effect of On-Off Operating Schedule

The schedule of system operation is studied as to its influence on the use of thermal heat storage and of possible off-peak rates for energy. Keeping the same total daily energy consumption, the rate of electrical input into the heating system was varied in proportion to the length of time of operation. Based on the system at the experimental site, the total input required for a mat area of 35.6 ft² is equal to 7690 Btu/Day. This heat supply per day was used in the program to determine the heat losses (QE and QB), building load (QF), and net storage for a 24-hour period, as shown in Table 7.

The model results are based on an average outside air temperature of 30.7°F (-1°C). The mat temperatures reported are for the end of the operating period. Inside air temperatures are listed by their maximum values, along with the hour they occurred, as well as their values at the end of the day. Similarly, the slab temperatures are listed by their maximum values and the hour they occurred. Temperatures at 3 foot and 6 foot depth are chosen at their maximum values. Time lags are determined by the difference between the end of operating hours and the hours that temperatures reached their maximum values as listed in Table 7.

From computed results, the heat losses (QB and QE) and building load (QF) are essentially constant, independent of the operating period heat per hour as well as heat storage in rejecting state. The storage rates, both positive and negative, vary significantly with the changes of heat input rate. A higher heat input rate gives a greater storage level. However, the flow from storage is correspondingly large. In other words, the difference between heat absorbed and heat released by heat storage is only slightly influenced by

TABLE 7

HEAT FLOW AND TEMPERATURE CHARACTERISTICS AT DIFFERENT RATES OF HEAT INPUT

operating schedule. For instance, net storage at the rate of 54 Btu/hr ft² is 2642 Btu/Day, compared with 2699 Btu/Day when the heat rate is 9 Btu/hr ft² -- 2% difference. However, the hours at which the inside temperatures reached their maximum values are significantly different.

From Table 7, the maximum temperatures of inside air and slab rise more quickly when using higher heat input rate to the system due to the higher temperatures at the mat. Consequently, the time for system operation can be selected by varying heat input rate in order to obtain the greatest heat transfer to the building at approximately the coldest hour during occupied hours.

Effect of Climate Condition

The influence of daily average ambient temperature was determined over a range from a very cold day ($-10^{\circ}\text{F} \sim -23.3^{\circ}\text{C}$) to a warm day ($40^{\circ}\text{F} \sim 4.4^{\circ}\text{C}$). The influence of ambient temperature is determined for all heat flows. These consist of building load (QF), earth heat loss (QB), edge heat loss (QE), and heat storage (QS) -- receiving and rejecting.

The study is based on the existing conditions of the experimental site. Roof insulation had a R-value of 30 (hr ft² °F/Btu). Wall insulation had a R-value of 13. Foundation insulation had a R-value of 6. The building was assumed to be on-grade with a constant heat input rate (Heat = 13.5 Btu/ft² hr) supplied to the heating system for 16 hours, and then turned off for 8 hours.

The model results are presented in Figure 26. The model is run for a 24-hour period for each constant ambient air temperature mentioned above. Additionally, some ambient air temperatures were set to vary hourly to represent a typical 24-hour period pattern of variation.

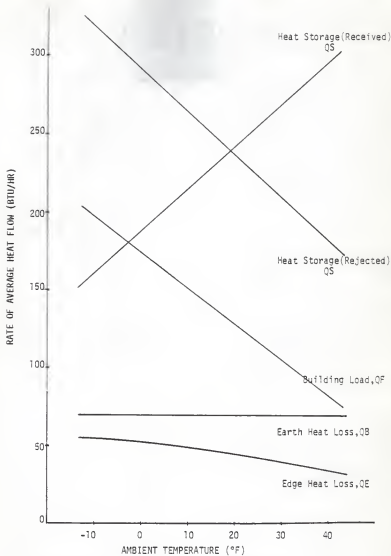


Figure 26. Heat Flow Pattern of Climate Condition.

The heat flow results are shown in Figure 26 as functions of ambient temperatures. Heat storage consists of two parts. Received heat storage is the heat obtained from a constant heat input when the heating system is operating for 16 hours. Rejected heat storage is the heat released from storage to earth and edge losses, and to building load as well as heat storage (surplus) remaining when the system turns off for an 8 hour period.

When the ambient temperature raises from a bitterly cold day ($-10^{\circ}\text{F} \sim -23.3^{\circ}\text{C}$) to a warm day ($40^{\circ}\text{F} \sim 4.4^{\circ}\text{C}$), the building load (QF) decreases significantly. Similarly, the rejected heat storage (QS) decreases due to reduced heat losses through building and its edge. The rate of building load decreases as outside temperature increases about $2.3 \text{ Btu}/^{\circ}\text{F}$. The rate of rejected heat storage is $2.7 \text{ Btu}/^{\circ}\text{F}$ which is about the same as the rate of received heat storage. The difference of the above heat rates ($0.4 \text{ Btu}/^{\circ}\text{F}$) is the rate of edge heat loss. The earth heat loss (QB) is totally unaffected by the change of ambient temperature. More heat is reserved in storage when the weather is warmer in the winter season.

The results listed in Table 8 were obtained by beginning each 24-hour computation at the "End of previous day" conditions: building temperature ($\text{TB}=70^{\circ}\text{F}$), floor temperature ($\text{TF}=72.3^{\circ}\text{F}$), inside air temperature ($\text{TI}=71.0^{\circ}\text{F}$), mat temperature ($\text{Tmat}=75.8^{\circ}\text{F}$) and 3 foot depth temperature ($\text{T3}'=72.1^{\circ}\text{F}$). The computed results show that TB, TF, and TI drop continuously to lower values for ambient temperature of -10°F and 0°F . The reduction is less at the outside temperatures beginning with 10°F . When outside temperature is 40°F , TB, TF, and TI increase from the starting value.

A change of outside temperature does not affect the mat temperature and the 3 foot deep soil temperatures. Of course, there is no effect at all on deeper soil temperatures at any outside temperature in short periods such as

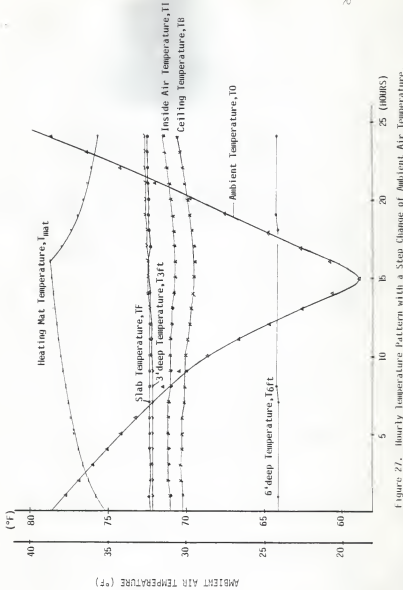


Figure 21. Hourly temperature pattern with a step change of ambient air temperature.

TABLE 8
TEMPERATURE PATTERN AT VARIOUS AMBIENT AIR TEMPERATURES

Ambient Temperature To (%)	Bldg Temperature TB (°F) @ Hour	Slab Temperature TF (°F) @ Hour	Inside Temperature TI (°F) @ Hour	Mat Temperature Tmat (°F) @ Hour	3 Foot Temperature T3' (°F) @ Hour
End of previous Day (30.7)	70.0	24	71.0	24	75.8
-10	65.9	24	70.3	24	79.7
0	66.8	24	70.6	24	79.8
10	68.0	10	71.3	13	79.8
Max.	---	---	71.4	17	79.8
20	68.9	10	71.8	8	79.9
Max.	69.0	14	71.9	16	79.9
Min.	69.9	2	72.1	6	79.9
30	70.4	21	72.7	21	79.9
40	71.5	24	73.4	24	80.0

one week.

From a winter average ambient temperature ($-30.7^{\circ}\text{F} \sim -1^{\circ}\text{C}$) typical of Kansas, the hourly ambient temperature variation does not affect the inside building temperatures, as is shown in Figure 27. From comparing two computed results, one used hourly varying ambient temperatures and one with constant daily average ambient temperature, slightly higher temperatures TB and TF, but lower temperature TI, are found for the hourly varying ambient temperature. As a result, building load and edge loss vary from 90 to 132 Btu/hr and from 39 to 43 Btu/hr respectively compared with steady building load (106 Btu/hr) and edge loss (40 Btu/hr) from the constant temperature assumption.

In Figure 27 it is shown that TB and TI dropped only slightly with the ambient temperature drop. Neglecting this small change, the use of a daily average ambient temperature is as good as using hourly varying ambient temperatures to study the heat flows of the system.

CHAPTER VI

SUMMARY AND CONCLUSION

From the analysis and comparison presented in the previous chapters, the model developed for two-dimensional, transient, finite difference program can be used as a tool for analyzing heat flow and temperature characteristics of a typical one-story building in areas similar to Kansas in climate and soil properties.

The Gauss-Seidel method (12) was used to solve the transient two-dimensional heat transfer finite difference equations in an explicit form. A variable time step iteration technique was used along with this method due to the dissimilar nature of the equations for surface and interior nodes.

The results of the model determining heat flows and temperatures were compared to the results of measured heat flows and temperatures for an early fall day and a late winter day. The model was shown to be reliable for use when computed and measured results were compared on an early fall day. However, the comparison of results showed less reliable results for heat flows and temperatures for a late winter day.

The model was used to study the effects of soil properties, building thermal transmittance, edge insulation thickness, building embankment, heat input intensity, on-off operating schedule, and climate conditions. The results of these parameters are presented in the form of Tables and Figures.

For a designated air temperature of building, the heat input required can be selected using the results under climate condition as a function of

building thermal transmittance, edge insulation thickness, and embankment, if applicable. However, if the design air temperature is not satisfactory, a change in heat input intensity may be required. The result of the operating schedule study may be used to determine a convenient operating period for matching the heat load to a favorable electrical rate. The soil properties study can be used as a guide to determine whether or not to use insulation beneath the sand bed, and to determine time lag of heat flows as a function of sand properties. With the aid of weather forecasts and data, and using the heat input intensity of the system, one can control the heating load to produce the most efficient system for human comfort.

The ultimate purpose of this paper was to develop a model that could be easily changed to adapt to other values for a parametric study of design options.

LIST OF REFERENCES

1. American Society of Heating, Refrigerating, and Air Conditioning Engineers, Inc., "Survey of Thermal Energy Storage Installations in the United States and Canada." ASHRAE Bulletin ISBN 0-910110-37-9, 1984.
2. Kusuda, Tamami, and Achenbach, P. Reece, "Earth Temperatures and Thermal Diffusivity at Selected Station in the United States." ASHRAE Transaction, Vol. 71, Part 1, 1965, pp. 61-73.
3. Van Gerpen, J.H., and Shapiro, H.N., "Analysis of Slab Heated Buildings." Engineering Research Institute, Iowa State University, Ames, Iowa, Report No. 2378, December 1984.
4. Szydlowski, R.F., "Analysis of Transient Heat Loss in Earth-Sheltered Structures." Underground Space, 5: N. 4, January 1981, pp. 237-246.
5. Shipp, P.H.; Pfender, E.; and Bligh, T.P.; "Thermal Characteristics of a Larger Earth-Sheltered Building." Underground Space, 6: No. 1, July 1981, pp. 53-64.
6. Shen, L.S., and Ramsey, J.W., "A Simplified Thermal Analysis of Earth-Sheltered Buildings Using a Fourier-Series Boundary Method." ASHRAE Transaction, Vol. 89, Part 1B, 1983, pp. 438-448.
7. Cheng, H.S.Y., and Orucker, E.E., "Analog Study of Heating in Survival Shelters." ASHRAE Symposium on Survival Shelters, June 25-27, 1962, pp. 35-80.
8. Kusuda, T., and Achenbach, P.R., "Numerical Analysis of the Thermal Environment of Occupied Underground Spaces with Finite Cover Using a Digital Computer." ASHRAE Transaction, Vol. 69, 1963, pp. 439-452.
9. Wang, F., "Mathematical Modeling and Computer Simulations of Insulated System in Below Grade Applications." Proceedings of the ASHRAE/OOE Conference on Thermal Performance of the Exterior Envelope of Buildings, ASHRAE, New York, 1979, pp. 457-471.
10. Oelsante, A.E.; Stokes, A.N.; and Walsh, P.J., "Application of Fourier Transforms to Periodic Heat Flow into the Ground Under a Building." International Journal of Heat and Mass Transfer, Vol. 26, January-June, 1983, pp. 121-132.
11. Duffie, J.A., and Beckman, W.A., Solar Engineering of Thermal Process, Chapters 3,4, & 6, John Wiley & Sons, New York, 1980.

LIST OF REFERENCES

(Continued)

12. Karlekar, V.B., and Desmond, M.R., Engineering Heat Transfer, Chapter V, West Publishing Company, New York, New York, 1980.
13. Billington, Neville S., "Heat Loss Through Solid Ground Floors." Institution of Heating and Ventilating Engineers, Vol. 19, November 1951, pp. 351-372.
14. American Society of Heating, Refrigerating, and Air Conditioning Engineers, Inc., ASHRAE Handbook of Fundamentals, New York, New York, 1981, pp. 5.9, 23.14, 23.15.
15. Jumikis, Alfred R., Thermal Soil Mechanics, Rutgers University Press, New Brunswick, New Jersey, 1966, p. 231.
16. Kreith, Frank, Principles of Heat Transfer, 2nd ed., International Textbook Company, Scranton, Pennsylvania, 1969, p. 593.
17. Hoagland, L.C., A Thermal Engineering Study of the Smith-Gates Deepheat System, Farmington, Connecticut, 1970, pp. 1-23.

APPENDIX A

LIST OF SYMBOLS

APPENDIX A

LIST OF SYMBOLS

<u>Symbol</u>	<u>Description</u>	<u>Units</u>
AB	Building area	ft ²
AF	Floor area	ft ²
ANFA, α	Thermal diffusivity of soil	ft ² /day
AR	Roof area	ft ²
AS	Annual earth surface temperature amplitude	°F
ASO	Annual amplitude of air temperature	°F
AW	Total wall area	ft ²
AWC	Concrete wall area	ft ²
AWI	Insulated wall area	ft ²
BROAD	Width of building	ft
CP	Heat capacity	Btu/Lbm F
CPF	CP: heat capacity, F: floor concrete	Btu/Lbm F
D	Density of element	Lbm/ft ³
DATE	Day number of the date in the year	days
DC(f)	Product of density and heat capacity at node (f)	Btu/ft ³ F
DELTA, Δt_1	Time increment of the building part	hr
Δt	Time interval	hr
DELTIM, Δt_2	Time increment of the soil part	hr
DELXI	Grid horizontal dimension (ΔX) indoor	ft
DELXD	Grid horizontal dimension (ΔX) outdoor	ft

APPENDIX A

(Continued)

<u>Symbol</u>	<u>Description</u>	<u>Units</u>
DELX1, DELX2	Grid horizontal dimension indoor and outdoor respectively	in
DELY	Grid vertical dimension	ft
DELY1	Grid vertical dimension	in
FIT	Footing insulation thickness	ft
FLT	Floor thickness	ft
FNOD	Number of footing nodes	none
FT	Footing thickness	ft
HF	Height of footing	in
HI	Height of footing insulation	in
HIC ₁ , H ₂ , HIC ₂	Convective coefficient on horizontal plate	Btu/hr ft ² F
HIW, H ₁ , HIW ₂	Convective coefficient on vertical plate	Btu/hr ft ² F
HO	Outside air convective coefficient for winter	Btu/hr ft ² F
HR, HR ₂	Radiative coefficient of floor to roof	Btu/hr ft ² F
MB	Mass of building - roof and wall	lb
Q	Building loss	Btu/hr
QB	Bottom loss to the earth	Btu/hr
QE	Edge loss through side of building	Btu/hr
QF	Heat gain by building from floor	Btu/hr
QHEAT	Heat input or internal heat generation per mat area	Btu/hr ft ²
QL	Heat input or heat rejection	Btu/hr
QLOAD, Q1	Heat loss through building wall and ceiling	Btu/hr

APPENDIX A

(Continued)

<u>Symbol</u>	<u>Description</u>	<u>Units</u>
QLOAD1, Q2	Heat loss through embankment	Btu/hr
QS	Heat storage in sand bed	Btu/hr
RC	Concrete thermal resistance	hr ft ² F/Btu
RCB	Product of density and heat capacity of building	Btu/ft ³ F
RCR(f)	Product of density and heat capacity of roof	Btu/ft ³ F
RCWST	Product of density and heat capacity of building wall	Btu/ft F
RI	Inside air resistance for vertical surface	Btu/hr ft ² F
RIR	Roof insulation resistance (R-value)	Btu/hr ft ² F
RIT	Roof insulation thickness	ft
RIW	Wall insulation resistance	Btu/hr ft ² F
RO	Outside air resistance	Btu/hr ft ² F
ROF	Density of material where F is floor concrete; A: air, C: wall concrete, I: footing insulation, R: roof insulation, S: soil, SD: sand, ST: steel, W: wall insulation	Lb/ft ³
RR	Roof thermal resistance	hr ft ² F/Btu
RRF	Roof inside air resistance for horizontal surface	hr ft ² F/Btu
RT	Total roof thickness	ft
RWC	Concrete wall thermal resistance	hr ft ² F/Btu
RWI	Insulated wall thermal resistance	hr ft ² F/Btu
S(XX)	Soil berm temperature	°F
SCT	Sand and floor concrete thickness (depth)	in

APPENDIX A
(Continued)

<u>Symbol</u>	<u>Description</u>	<u>Units</u>
SDNOD	Number of sand nodes	none
SIM _A , σ	Stefan-Boltzmann constant	Btu/hr ft ² °R ⁴
STT	Steel wall thickness	ft
t	Time	hr
T(XX) or TT(XX)	Earth temperature at designated node or depth	°F
TA or T0	Ambient (outside) air temperature	°F
TB or TT _B	Building inner roof surface average temperature	°F
TC(i)X or Y	Thermal conductivity at node (i) by X or Y direction	Btu/hr ft F
TCF	Thermal conductivity where F is floor concrete; (see listing ROF)	Btu/hr ft F
TCL	Thermal conductivity of building wall	Btu/hr ft F
TCR	Roof thermal conductivity	Btu/hr ft F
TF	Average floor temperature	°F
THETA, φ	Phase angle of annual cycle	Radian
TI	Inside building temperature	°F
TIL	Total insulated roof and wall length	ft
TMA	Annual average air temperature	°F
TMS	Annual average soil temperature	°F
TWI, TWI ₂	Inside wall surface average temperature	°F
TWO, TWO ₂	Outside wall surface average temperature	°F
UB	Average thermal transmittance of building	Btu/hr ft ² F
UR	Roof thermal transmittance	Btu/hr ft ² F

APPENDIX A

(Continued)

<u>Symbol</u>	<u>Description</u>	<u>Units</u>
UWC	Concrete wall thermal transmittance	Btu/hr ft ² F
UWI	Insulated wall (U-value) thermal transmittance	Btu/hr ft ² F
VAIR	Volume of inside air of building	ft ³
VB	Building volume by roof and wall	ft ³
WCH	Wall concrete height	ft
WCT	Wall concrete thickness	ft
WIH	Wall insulation height	ft
WIT	Wall insulation thickness	ft
WT	Wall thickness	ft
Y	Depth of the soil from soil surface	ft

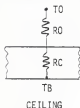
APPENDIX B
LIST OF AUXILIARY EXPRESSIONS

APPENDIX B

DETAILS OF AVERAGE VALUES

U-Value of Building

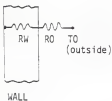
Building thermal transmittance is combined by an average calculation between roof and wall thermal transmittances.



$$R_{ROOF} = RC + RO \text{ where } AR: \text{Roof area}$$

$$U_{ROOF} = 1/R_{ROOF}$$

CEILING



$$R_{WALL} = RW + RO \text{ where } AW: \text{Wall area}$$

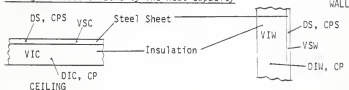
$$U_{WALL} = 1/R_{WALL}$$

WALL

COMBINATION

$$UB = (AR \cdot U_{ROOF} + AW \cdot U_{WALL}) / (AR + AW)$$

Average Product of Density and Heat Capacity



APPENDIX B

(Continued)

where:

VIC: Insulated ceiling volume

VIW: Insulated wall volume

VSC: Steel sheet volume

Building product of density and heat capacity is given:

$$DB \cdot CPB = (VIW \cdot DIW \cdot CP + VIC \cdot DIC \cdot CP + VSC \cdot DS \cdot CPS) / (VIW + VIC + VSC)$$

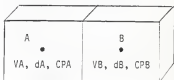
A similar method is applied to evaluate the average value between two different material adjacent nodes for average product D·CP.

where:

VA, VB : Volume of each node

dA, dB : Density

CPA, CPB: Heat capacity

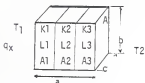


$$D \cdot CP = (VA \cdot dA \cdot CPA + VB \cdot dB \cdot CPB) / (VA + VB)$$

If element A or B contains more than one material property, then the products of density and heat capacity of each element would be averaged by each material before heat flow calculation.

Average Thermal Conductivity Method

The principle of calculated thermal conductivity is generally applied in series or parallel thermal conductivity.



where:

K: Thermal conductivity

L: Thickness

A: Cross section area

APPENDIX B

(Continued)

Series case (heat flows in x direction)

$$T_1 \xrightarrow{\text{---}} \text{---} \xrightarrow{\text{---}} \text{---} \xrightarrow{\text{---}} T_2$$

$\frac{L_1/K_1 \cdot A_1}{A_1} \quad \frac{L_2/K_2 \cdot A_2}{A_2} \quad \frac{L_3/K_3 \cdot A_3}{A_3}$

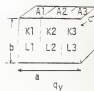
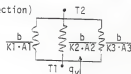
where: $A = A_1 = A_2 = A_3 = bc$, $\Delta x = a$

$$\Rightarrow K_S = \Delta x / (L_1/K_1 + L_2/K_2 + L_3/K_3)$$

Parallel case (heat flows in y direction)

$$q_y = K_P \cdot \Delta \cdot (\Delta T / \Delta y)$$

$$q_y = \Delta T / [1/(b/K_1 \cdot A_1) + 1/(b/K_2 \cdot A_2) + 1/(b/K_3 \cdot A_3)]^{-1}$$



$$= \Delta T / [1/(b/K_1 \cdot L_1 \cdot c) + 1/(b/(K_2 \cdot L_2 \cdot c)) + 1/(b/(K_3 \cdot L_3 \cdot c))]^{-1}$$

where:

$$A_1 = L_1 \cdot c$$

$$= \Delta T / [(c/b) \cdot (K_1 \cdot L_1 + K_2 \cdot L_2 + K_3 \cdot L_3 + c)]^{-1}$$

$$A_2 = L_2 \cdot c$$

$$= (c/b) \cdot (K_1 \cdot L_1 + K_2 \cdot L_2 + K_3 \cdot L_3) \cdot \Delta T$$

$$A_3 = L_3 \cdot c$$

$$\text{yields: } (K_1 \cdot L_1 + K_2 \cdot L_2 + K_3 \cdot L_3) = K_P \cdot A / \Delta y$$

$$A = c(L_1 + L_2 + L_3) = ca$$

$$= K_P \cdot a$$

L : Thickness

$$K_P = (K_1 \cdot L_1 + K_2 \cdot L_2 + K_3 \cdot L_3) / a$$

Differential Equations in Heat Transfer

Fourier's Law is applied for heat conduction:

$$Q_n = -K \cdot A \cdot (\Delta T / \Delta n) \text{ in } n\text{-direction}$$

where:

 $\Delta T / \Delta n$ = the temperature gradient in the n -direction A = the area normal to the n -direction

$$Q_n = \text{the total heat flow through } A$$

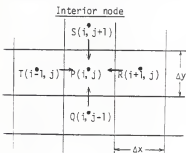
APPENDIX B

(Continued)

Integrating for Δn -interval distance yields:

$$Q = -K \cdot A \cdot (\Delta T / \Delta n)$$

Heat flows of transient two-dimensional heat conduction are analyzed on elements and nodes as shown below.



$$\begin{aligned} Q_{T \rightarrow P} &= K_{i-1} (\Delta y \cdot 1) \cdot (T_{i-1,j} - T_{i,j}) / \Delta x \\ Q_{R \rightarrow P} &= K_{i+1} (\Delta y \cdot 1) \cdot (T_{i+1,j} - T_{i,j}) / \Delta x \\ Q_{Q \rightarrow P} &= K_{j-1} (\Delta x \cdot 1) \cdot (T_{i,j-1} - T_{i,j}) / \Delta x \\ Q_{S \rightarrow P} &= K_{j+1} (\Delta x \cdot 1) \cdot (T_{i,j+1} - T_{i,j}) / \Delta x \\ \Delta U_{i,j} &= D \cdot C_P \cdot (\Delta x \cdot \Delta y \cdot 1) \cdot (T_{i,j}^* - T_{i,j}) / \Delta t \end{aligned}$$

Conservation of energy:

$$Q_{T \rightarrow P} + Q_{R \rightarrow P} + Q_{Q \rightarrow P} + Q_{S \rightarrow P} = \Delta U_{i,j}$$

In heat transfer form:

$$K_{i-1} \cdot \Delta y \cdot (T_{i-1,j} - T_{i,j}) / \Delta x + K_{i+1} \cdot \Delta y \cdot (T_{i+1,j} - T_{i,j}) / \Delta x + K_{j-1} \cdot \Delta x \cdot (T_{i,j-1} - T_{i,j}) / \Delta y + K_{j+1} \cdot \Delta x \cdot (T_{i,j+1} - T_{i,j}) / \Delta y = D \cdot C_P \cdot (\Delta x \cdot \Delta y) \cdot (T_{i,j}^* - T_{i,j}) / \Delta t$$

Explicit form:

$$T_{i,j}^* = \Delta t / D \cdot C_P \cdot (\Delta x \cdot \Delta y) \cdot [K_{i-1} \cdot \Delta y \cdot (T_{i-1,j} - T_{i,j}) / \Delta x + K_{i+1} \cdot \Delta y \cdot (T_{i+1,j} - T_{i,j}) / \Delta x + K_{j-1} \cdot \Delta x \cdot (T_{i,j-1} - T_{i,j}) / \Delta y + K_{j+1} \cdot \Delta x \cdot (T_{i,j+1} - T_{i,j}) / \Delta y] + T_{i,j}$$

where:

$T_{i,j}^*$: Future temperature after Δt time elapses at (i,j) th node (F)

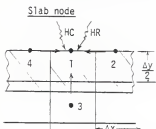
Δt : Time elapses from (t) to $(t + \Delta t)$ (hr)

D: Density of element (Lbm/ft^3)

APPENDIX B

(Continued)

CP: Heat capacity of element (Btu/Lbm F)

 Δx : x-dimension of element (ft) Δy : y-dimension of element (ft) K_{i-1} : Thermal conductivity from T to P node (Btu/hr ft F) $T_{i-1,j}$: Temperature of $(i-1,j)^{\text{th}}$ node at time t (F)

$$Q_{HC+1} = HC \cdot (\Delta x + 1) \cdot (T_1 - T_1)$$

$$Q_{HR+1} = HR \cdot (\Delta x + 1) \cdot (T_2 - T_1)$$

$$Q_{2 \rightarrow 1} = K_2 \cdot ((\Delta y/2) + 1) \cdot (T_2 - T_1) / \Delta x$$

$$Q_{3 \rightarrow 1} = K_3 \cdot ((\Delta y/2) + 1) \cdot (T_3 - T_1) / \Delta x$$

$$Q_{4 \rightarrow 1} = K_4 \cdot (\Delta x + 1) \cdot (T_4 - T_1) / \Delta y$$

$$\Delta U = D \cdot CP \cdot (\Delta x \cdot (\Delta y/2) + 1) \cdot (T^{*1} - T_1) / \Delta t$$

Conservation of energy:

$$Q_{HC+1} + Q_{HR+1} + Q_{2 \rightarrow 1} + Q_{3 \rightarrow 1} + Q_{4 \rightarrow 1} = \Delta U$$

Heat transfer form:

$$HC \cdot \Delta x \cdot (T_1 - T_1) + HR \cdot \Delta x \cdot (T_2 - T_1) + K_2 \cdot (\Delta y/2) \cdot (T_2 - T_1) / \Delta x + K_3 \cdot \Delta x \cdot (T_3 - T_1) / \Delta y + K_4 \cdot (\Delta y/2) \cdot (T_4 - T_1) / \Delta x = \rho \cdot CP : D \cdot CP \cdot (\Delta x \cdot (\Delta y/2)) \cdot (T^{*1} - T_1) / \Delta t$$

Temperature distribution:

$$T^{*1} = (2 \Delta t / D \cdot CP \cdot \Delta x \cdot (\Delta y/2)) [HC \cdot \Delta x \cdot (T_1 - T_1) + HR \cdot \Delta x \cdot (T_2 - T_1) + K_2 \cdot (\Delta y/2) \cdot (T_2 - T_1) / \Delta x + K_4 \cdot (\Delta y/2) \cdot (T_4 - T_1) / \Delta x + K_3 \cdot \Delta x \cdot (T_3 - T_1) / \Delta y] + T_1$$

where:

 T^{*1} : Future temperature of node #1 at time $(t + \Delta t)$ (F) Δt : Time increment (hr)

APPENDIX B

(Continued)

D: Density (Lbm/ft³)

CP: Heat capacity (Btu/Lbm F)

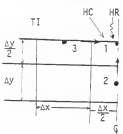
 Δx : x-dimension of element (ft) Δy : y-dimension of element (ft)HC: Convective coefficient (Btu/hr ft² F)HR: Radiative coefficient (Btu/hr ft² F)

TI: Inside air temperature (F)

T1: Temperature of node #1 at time t

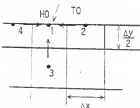
TB: Inside surface ceiling temperature (F)

K2: Thermal conductivity from node #2 to node #1 (Btu/hr ft F)

Slab corner node

Similarly, temperature distribution is:

$$T^*1 = [\Delta t/D + CP \cdot (\Delta x/2) \cdot (\Delta y/2)] \cdot [HC \cdot (\Delta x/2) \cdot (TI - T1) + HR \cdot (\Delta x/2) \cdot (TB - T1) + K2 \cdot (\Delta x/2) \cdot (T2 - T1)/\Delta y + K3 \cdot (\Delta y/2) \cdot (T3 - T1)/\Delta x] + T1$$

Soil surface node

$$T^*1 = [\Delta t/D + CP \cdot \Delta x \cdot (\Delta y/2)] \cdot [HO \cdot \Delta x \cdot (TO - T1) + K2 \cdot (\Delta y/2) \cdot (T2 - T1)/\Delta x + K3 \cdot (\Delta y/2) \cdot (T4 - T1)/\Delta x + K3 \cdot \Delta x \cdot (T3 - T1)/\Delta y] + T1$$

APPENDIX B
(Continued)

Soil surface corner node

$$T^*(o,t) = TMS - AS \cdot \cos((2\pi n/365) + B)$$

where:

$T^*(o,t)$: Soil temperature at surface (depth = o ft) and time t (F)

TMS: Annual average soil temperature (F)

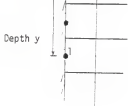
AS: Annual earth surface temperature amplitude (F)

n: Days of the year (Day)

B: Phase angle of annual cycle (Rad)

Note that $T^*(o,t)$ depends only on t, other parameters are constant.

Undisturbed soil temperature boundary node



$$T^*l = TMS - AS \cdot \exp(-y \cdot \sqrt{\pi/365} \cdot \Delta) \cdot \cos(2\pi n/365 - y\sqrt{\pi/365} \cdot \Delta - B)$$

where

T^*l : Undisturbed soil temperature at depth y (F)

Δ : Thermal diffusivity (ft^2/Day)

y: Depth of soil (ft)

Other symbols, see above.

Also, the undisturbed soil temperature at two corner boundary nodes at depth of 10.5' is calculated by the above expression. This undisturbed soil temperature is used to assume the bottom boundary conditions at depth of 10.5'.

Uninsulated boundary node

Δy	$\Delta x/2$	4*
		3
		1*

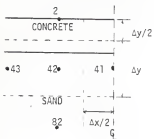
$$T^*l = \frac{\Delta t / D \cdot C_p \cdot \Delta z \cdot (\Delta x / 2) \cdot \Delta y}{[\Delta x \cdot K_2 \cdot (\Delta x / 2) \cdot (T_2 - T_1) + \Delta y \cdot K_3 \cdot \Delta y \cdot (T_3 - T_1) / \Delta x + \Delta y \cdot K_4 \cdot (\Delta x / 2) \cdot (T_4 - T_1) / \Delta y]} + T_1 \quad (\text{Note: } \Delta z \text{ is unity for all nodes.})$$

APPENDIX B

(Continued)

Some Particular Nodes (Sample)

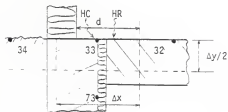
Node 42, heterogeneous node



$$T^{*42} = (\Delta t / D \cdot CP \cdot \Delta x \cdot \Delta y) [K41 \cdot \Delta y \cdot (T41 - T42) / \Delta x + K43 \cdot \Delta y \cdot (T43 - T42) / \Delta x + KB2 \cdot \Delta x \cdot (T82 - T42) / \Delta y + K2 \cdot \Delta x \cdot (T2 - T42) / \Delta y] + T42$$

(D-CP), K41, and K2 are calculated as in previous section for their average values.

Node 33



$$T^{*33} = (\Delta t / D \cdot CP \cdot \Delta x \cdot (\Delta y / 2)) \cdot [HC \cdot d \cdot (TI - T33) + HR \cdot d \cdot (TB - T33) + K32 \cdot (\Delta y / 2) \cdot (T32 - T33) / \Delta x + K34 \cdot (\Delta y / 2) \cdot (T34 - T33) / \Delta x + K73 \cdot \Delta x \cdot (T73 - T33) / \Delta y] + T33$$

All K's are evaluated using the method of the previous section for their average values as well as product of (D·CP). d is surface area that remained after element surface was covered partially by wall.

Stability Criterion

Upperslab expressions

Inside air temperature expressions:

APPENDIX B

(Continued)

$$TI^* = (\Delta t/VAIR\cdot OA\cdot CPA) \cdot [AR\cdot H2 \cdot (TB - TI) + AW\cdot H1 \cdot (TB - TI) + AF\cdot H2 \cdot (TF - TI)] \\ + TI$$

$$TI^* = (\Delta t/VAIR\cdot OA\cdot CPA) \cdot [(AR\cdot H2 + AW\cdot H1)\cdot TB + AF\cdot H2\cdot TF - (AR\cdot H2 + AW\cdot H1 + AF\cdot H2)\cdot TI] + TI$$

$$\text{Let } a = (\Delta t/VAIR\cdot OA\cdot CPA) \cdot (AR\cdot H2 + AW\cdot H1 + AF\cdot H2)$$

For TI terms of no-berm case

$$-a \cdot TI + TI = (1 - a) \cdot TI$$

If $(1 - a) < 0 \Rightarrow$ fluctuating values of temperatures (reference 12)

Result, $1 - a > 0$ or $a < 1$

$$\text{then } \Delta t < VAIR\cdot OA\cdot CPA / (AR\cdot H2 + AW\cdot H1 + AF\cdot H2)$$

$$\text{where } AR\cdot H2 = 37.67(0.22(TB - TI))^{.33}$$

$$AW\cdot H1 = 17.25(0.19(TB - TI))^{.33}$$

$$AF\cdot H2 = 37.67(0.22(TF - TI))^{.33}$$

$$VAIR = 649.8, OA\cdot CPA = 0.0735 + 0.2406 = 0.01768$$

$$\text{If } TF = 75, TI = 73, TB = 72.0^\circ F,$$

$$\text{then: } \Delta t \leq (649.8 + 0.01768) / (8.287 + 3.277 + 10.441) \leq 0.52 \text{ hours}$$

Ceiling temperature expression:

$$TB^* = (\Delta t/VB\cdot OB\cdot CPB) \cdot [H2\cdot AR\cdot (TI - TB) + H1\cdot AW\cdot (TI - TB) + HR\cdot AF\cdot (TF - TB)] + UB\cdot AB\cdot (TO - TB) + TB$$

$$\text{Let } a = (\Delta t/VB\cdot OB\cdot CPB) \cdot (H2\cdot HR + H1\cdot AW + HR\cdot AF + UB\cdot AB)$$

$$\text{where: } AF\cdot HR = 37.67(0.1714 \cdot 10^{-8}) \cdot [(460 + TF)^4 - (460 + TB)^4] / (TF - TB)$$

$$\text{then: } \Delta t \leq VB\cdot OB\cdot CPB / (AR\cdot H2 + AW\cdot H1 + AF\cdot HR + AB\cdot UB)$$

$$\Delta t \leq 14.29 \cdot 1.26 / (8.287 + 3.277 + 39.177 + 2.581) \leq 0.34 \text{ hr}$$

APPENDIX B

(Continued)

Underslab expressions

Internal node:

Similarly, the temperature equation gives:

$$\Delta t \leq \Delta x \cdot \Delta y \cdot D \cdot CP / [(K_{j-1} + K_{j+1}) \cdot \Delta y / \Delta x + (K_{i-1} + K_{i+1}) \cdot \Delta x / \Delta y]$$

For i = 254; soil: K = 1.07, D·CP = 23.8 (see list of symbols for units)
 then, $\Delta t \leq 4.4$ hrs

For i = 90; sand: K = 1.28, O·CP = 21.2

then, $\Delta t \leq 3.8$ hrswhere: $\Delta x = 1.167$ ft, $\Delta y = 0.75$ ft

Slab node (concrete material):

$$\Delta t \leq \Delta x \cdot (\Delta y / 2) \cdot D \cdot CP / [(H_2 + HR) \cdot \Delta x + K_1 \cdot \Delta y / \Delta x + K_2 \cdot \Delta x / \Delta y]$$

where: O·CP = 29.4, K1 = 0.75, K2 = 0.87, H2 = 0.22, HR = 1.04
 then, $\Delta t \leq 3.7$ hrs

Soil surface node:

$$\Delta t \leq D \cdot CP \cdot \Delta x \cdot (\Delta y / 2) / [(H_0 \cdot \Delta x) + K_1 \cdot \Delta y / \Delta x + K_2 \cdot \Delta x / \Delta y]$$

where: H0 = 6, K1 = K2 = 1.07, D·CP = 23.8

then, $\Delta t \leq 1.14$ hrs

Summary of other nodes:

Node	Time limit, Δt (hour)
T(33)	5.00
T(1)	3.90
T(41)	1.95

APPENDIX B

(Continued)

Heat Flow Estimate of Existing Building

Figure 28 indicates measured temperatures as well as average measured temperatures. Shaded area is heat flow control limit for dealing with heat calculations. For instance, temperature T1 is the average of thermocouples TC15 and TC30, T8 is the average between T9 and T7, etc.

The calculated samples following are estimates of "measured" heat flows for November 12, 1984 at 8:00 a.m. only. Other dates and times for heat flow estimates are similar calculations.

Heat gain QF = QF1 + QF2: net heat gain for building. Where:

QF1 = K·A1·(T2 - TC15)/d1; assumed heat flow upward of slab

K = concrete thermal conductivity = 0.75 Btu/hr ft F

A1 = partial floor area (assumed for heat flow upward) = 34.5 ft²

T2 = concrete temperature by averaging = 73.5 F, [(TC30 + TC15)/2 = T1,
T2 = (T1 + TC15)/2]

TC15 = temperature at thermocouple 15 = 71.9 F

d1 = path length of heat flow = 0.375 ft

QF2 = K·A2(TC13 - TC17)/d2

where: K = 0.75 Btu/hr ft F, A2 = 3 ft², TC13 = 67.9 F, TC17 = 67.4 F,

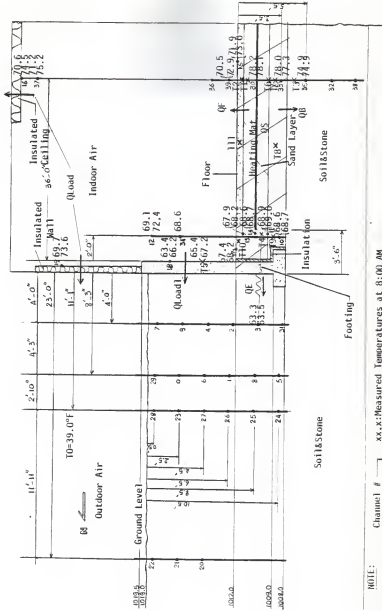
d2 = 0.5 ft

Heat loss to the bottom: QB = KS·A·(TC33 - T3)/d. Where:

KS: soil thermal conductivity = 1.07 Btu/hr ft F

A = 37.5 ft², d = 1 ft .

TCB3 = 78 F, T3 = 76.5 F



NOTE:

Channel # 1 xx.x: Measured Temperatures at 8:00 AM

Thermocouple Location 36 xx.x: Measured Temperatures at 4:00 PM

Figure 28. Temperature Configuration for Measured Heat Flow Estimate.

APPENDIX B

(Continued)

Heat loss thru edge (4 ft deep): $QE = K_{avg} \cdot A \cdot (T4 - TC3)/d$.

Where: K_{avg} = average thermal conductivity = 0.55 Btu/hr ft F

$A = 4 \text{ ft}^2$, $d = 6.67 \text{ ft}$

$$T4 = (TC11 + TC14)/2 = 68.75 \text{ F}, TC3 = 63.6 \text{ F}$$

Heat storage: $QS = Q_{input} - (QF + Q8 + QE)$, or it can be calculated by weighted average method.

$$QS = \bar{m} \cdot \bar{CP} \cdot \Delta T = I_i m \cdot CP \cdot \Delta T \text{ for 8 hours}$$

Where: i = floor, sand, soil

\bar{m} : average mass

\bar{CP} : average heat capacity

ΔT : average temperature

Heat storage in concrete: $QC = V \cdot d \cdot CP \cdot (T11^* - T11) \quad (\text{Btu}/8 \text{ hrs})$

Where: V : concrete volume = 0.5 ft x 37.5 ft²

d : concrete density = 140 (Lbm/ft³)

CP : concrete heat capacity = 0.21 (Btu/Lbm F)

$$T11 = (T2 + (TC17 + TC13)/2)/2 = 70.6 \text{ F @ 8:00 a.m.,}$$

71.3 F @ 4:00 p.m.

Heat storage in sand: $QSO = V \cdot d \cdot CP \cdot (TC30^* - TC30) \quad (\text{Btu}/8 \text{ hrs})$

Where: $V = 2 \text{ ft} \times 37.5 \text{ ft}^2$

$d = 106 \text{ Lbm/ft}^3$

$CP = 0.2 \text{ Btu/Lbm F}$

$TC30 = 78.2 \text{ F, } 78.1 \text{ F}$

Heat storage in soil: $QSL = V \cdot d \cdot CP \cdot (T8^* - T8) \quad (\text{Btu}/8 \text{ hrs})$

Where: $V = 1.5 \text{ ft} \times 37.5 \text{ ft}^2$

APPENDIX B

(Continued)

$$d = 140 \text{ Lbm/ft}^3$$

$$C_p = 0.17 \text{ Btu/Lbm F}$$

$$T_8 = (T_7 + T_9)/2 = [(TC_{30} + TC_{33})/2 + TC_{33}]/2 + (TC_{12} + TC_{11})/2] = 74 \text{ F and } 73.5 \text{ F}$$

Total building loss: $Q_{Loss} = Q_{Load1} + Q_{Load2}$.

Heat loss through concrete wall; $Q_{Load1} = \text{Radiation} + \text{Convection}$

$$Q_{Load1} = [hc(TC_{10} - T_5) + hr(TC_{15} - TC_5)] \cdot A$$

Where: hc : convective coefficient = 0.307 Btu/hr ft² F

hr : radiative coefficient = 1.01 Btu/hr ft² F

$$TC_{10} = 68.6 \text{ F}, T_5 = (TC_{18} + TC_{17})/2 = 65.4 \text{ F}$$

$$A = 7.5 \text{ ft}^2$$

Heat loss through building wall; $Q_{Load2} = UW \cdot A_1 \cdot (TC_{19} - T_0) + UR \cdot A_2 \cdot (TC_{16} - T_0)$

Where: UW : wall thermal transmittance = 0.076 Btu/hr ft² F

UR : roof thermal transmittance = 0.033 Btu/hr ft² F

$$A_1 = 9.75 \text{ ft}^2$$

$$A_2 = 37.5 \text{ ft}^2$$

$$T_0 = 39 \text{ F}$$

$$TC_{19} = 69.7 \text{ F}$$

$$TC_{16} = 70.6 \text{ F}$$

APPENDIX C

COMPUTER PROGRAM

```

FILE: LEVEL      MATRIX  A      KANSAS STATE UNIVERSITY VM/SP CMS
C   THE   AGES = 50
C   THE   N1
C   THE   N2
C   THE   N3
C   THE   N4
C   THE   N5
C   THE   N6
C   THE   N7
C   THE   N8
C   THE   N9
C   THE   N10
C   THE   N11
C   THE   N12
C   THE   N13
C   THE   N14
C   THE   N15
C   THE   N16
C   THE   N17
C   THE   N18
C   THE   N19
C   THE   N20
C   THE   N21
C   THE   N22
C   THE   N23
C   THE   N24
C   THE   N25
C   THE   N26
C   THE   N27
C   THE   N28
C   THE   N29
C   THE   N30
C   THE   N31
C   THE   N32
C   THE   N33
C   THE   N34
C   THE   N35
C   THE   N36
C   THE   N37
C   THE   N38
C   THE   N39
C   THE   N40
C   THE   N41
C   THE   N42
C   THE   N43
C   THE   N44
C   THE   N45
C   THE   N46
C   THE   N47
C   THE   N48
C   THE   N49
C   THE   N50
C   THE   THE SYSTEM & BUILDING
C   THE   MIN=0.47, MAX=10.81, AVG=0.75. THE VALUES ARE ALL
C   THE   CONCRETE

```

FILET LEVEL WATERIV A KANSAS STATE UNIVERSITY VM/SP CMS

CPC=CPS
C INSULATING MATERIALS PROPERTY DATA C 4 68 R
C FOR DENSITY DATA *****
C FOR THERMAL RESISTANCE DATA *****
C FOR CONDUCTIVITY DATA *****
C FOR PERMEABILITY DATA *****
C FOR SOIL PROPERTIES DATA *****
C MILD TEST AT 32F
C FOR SOIL PROPERTIES DATA *****
C FOR THERMAL RESISTANCE DATA *****
C FOR CONDUCTIVITY DATA *****
C FOR PERMEABILITY DATA *****
C ****AVERAGE DATA AT 60 F. NOTE RS IS THERMAL RESISTANCE
C ****FOR CONDUCTIVITY DATA *****
C ****FOR THERMAL RESISTANCE DATA *****
C ****FOR PERMEABILITY DATA *****
C ****FOR SOIL PROPERTIES DATA *****
C ****FOR INSULATING MATERIALS AND TEMPERATURE GRIDS *****
C ****FOR CONDUCTIVITY DATA *****
C ****FOR THERMAL RESISTANCE DATA *****
C ****FOR PERMEABILITY DATA *****
C ****FOR SOIL PROPERTIES DATA *****

FILE: LEVEL NATIVE & KANSAS STATE UNIVERSITY VM/SP CMS

KANSAS STATE UNIVERSITY LIBRARY CMS

1996-1997
1997-1998
1998-1999
1999-2000
2000-2001
2001-2002
2002-2003
2003-2004
2004-2005
2005-2006
2006-2007
2007-2008
2008-2009
2009-2010
2010-2011
2011-2012
2012-2013
2013-2014
2014-2015
2015-2016
2016-2017
2017-2018
2018-2019
2019-2020
2020-2021
2021-2022
2022-2023
2023-2024

W. H. STANLEY & CO., LTD.
10, BURTON STREET, MANCHESTER,
ENGLAND.

40

Now we can prove that $T(K) = T(K+1)$. We will do this by induction on K .

Base Case: For $K=1$, we have $T(1) = T(2)$ because $T(1) = \text{true}$ and $T(2) = \text{true}$. So the base case holds.

Inductive Step: Assume that $T(K) = T(K+1)$ for some $K \geq 1$. We want to show that $T(K+1) = T(K+2)$.

Consider the expression $\text{IF } K > 0 \text{ THEN } T(K) \text{ ELSE } T(K+1)$. By the definition of IF , this expression evaluates to $T(K)$ if $K > 0$ and $T(K+1)$ if $K \leq 0$.

Since $K \geq 1$, we have $K > 0$. Therefore, the expression evaluates to $T(K)$. By the inductive hypothesis, $T(K) = T(K+1)$. So the expression evaluates to $T(K+1)$.

Now consider the expression $\text{IF } K > 0 \text{ THEN } T(K+1) \text{ ELSE } T(K+2)$. By the definition of IF , this expression evaluates to $T(K+1)$ if $K > 0$ and $T(K+2)$ if $K \leq 0$.

Since $K \geq 1$, we have $K > 0$. Therefore, the expression evaluates to $T(K+1)$. By the inductive hypothesis, $T(K+1) = T(K+2)$. So the expression evaluates to $T(K+2)$.

Thus, we have shown that $T(K+1) = T(K+2)$. By induction, $T(K) = T(K+1)$ for all $K \geq 1$.

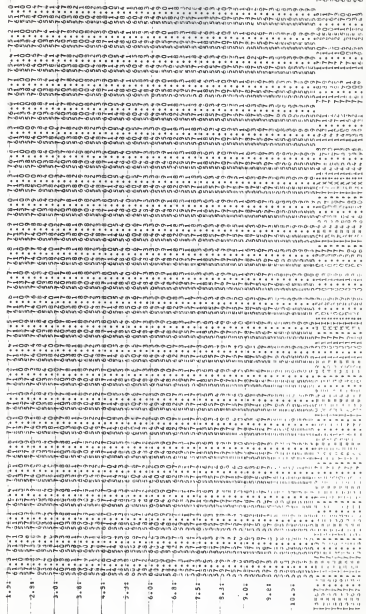
APPENDIX D

COMPUTER SAMPLE RESULTS FOR BERM AND NO-BERM

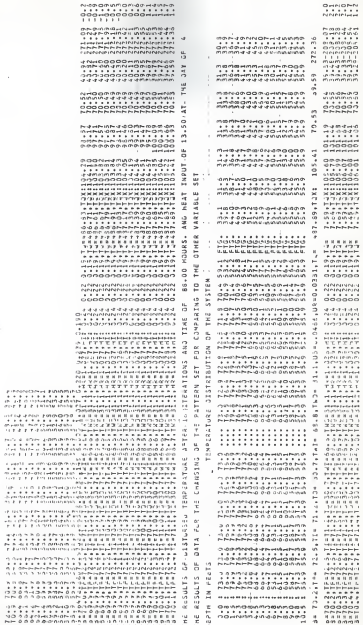
The figure displays a 16x16 grid representing temperature distribution. The columns are labeled with time steps: 0.0, 0.1, 0.2, 0.3, 0.4, 0.5, 0.6, 0.7, 0.8, 0.9, 1.0, 1.1, 1.2, 1.3, 1.4, 1.5, 1.6. The rows are labeled with depth levels: 0.0, 0.1, 0.2, 0.3, 0.4, 0.5, 0.6, 0.7, 0.8, 0.9, 1.0, 1.1, 1.2, 1.3, 1.4, 1.5, 1.6. The values in the grid range from approximately 0.0 to 1.0, with darker shades indicating higher temperatures.

Results Of Bern Case (Beginning With TB = 67.5)

Method of
Gauge
T = 0.020



Results of Beam Case (Ending At TB = 67.9)



Time	Distance	Speed	Acceleration	Deceleration
0.0	0.0	0.0	0.0	0.0
0.2	0.2	1.0	5.0	0.0
0.4	0.4	2.0	10.0	0.0
0.6	0.6	3.0	15.0	0.0
0.8	0.8	4.0	20.0	0.0
1.0	1.0	5.0	25.0	0.0
1.2	1.2	6.0	30.0	0.0
1.4	1.4	7.0	35.0	0.0
1.6	1.6	8.0	40.0	0.0
1.8	1.8	9.0	45.0	0.0
2.0	2.0	10.0	50.0	0.0
2.2	2.2	11.0	55.0	0.0
2.4	2.4	12.0	60.0	0.0
2.6	2.6	13.0	65.0	0.0
2.8	2.8	14.0	70.0	0.0
3.0	3.0	15.0	75.0	0.0
3.2	3.2	16.0	80.0	0.0
3.4	3.4	17.0	85.0	0.0
3.6	3.6	18.0	90.0	0.0
3.8	3.8	19.0	95.0	0.0
4.0	4.0	20.0	100.0	0.0
4.2	4.2	21.0	105.0	0.0
4.4	4.4	22.0	110.0	0.0
4.6	4.6	23.0	115.0	0.0
4.8	4.8	24.0	120.0	0.0
5.0	5.0	25.0	125.0	0.0
5.2	5.2	26.0	130.0	0.0
5.4	5.4	27.0	135.0	0.0
5.6	5.6	28.0	140.0	0.0
5.8	5.8	29.0	145.0	0.0
6.0	6.0	30.0	150.0	0.0
6.2	6.2	31.0	155.0	0.0
6.4	6.4	32.0	160.0	0.0
6.6	6.6	33.0	165.0	0.0
6.8	6.8	34.0	170.0	0.0
7.0	7.0	35.0	175.0	0.0
7.2	7.2	36.0	180.0	0.0
7.4	7.4	37.0	185.0	0.0
7.6	7.6	38.0	190.0	0.0
7.8	7.8	39.0	195.0	0.0
8.0	8.0	40.0	200.0	0.0
8.2	8.2	41.0	205.0	0.0
8.4	8.4	42.0	210.0	0.0
8.6	8.6	43.0	215.0	0.0
8.8	8.8	44.0	220.0	0.0
9.0	9.0	45.0	225.0	0.0
9.2	9.2	46.0	230.0	0.0
9.4	9.4	47.0	235.0	0.0
9.6	9.6	48.0	240.0	0.0
9.8	9.8	49.0	245.0	0.0
10.0	10.0	50.0	250.0	0.0
10.2	10.2	51.0	255.0	0.0
10.4	10.4	52.0	260.0	0.0
10.6	10.6	53.0	265.0	0.0
10.8	10.8	54.0	270.0	0.0
11.0	11.0	55.0	275.0	0.0
11.2	11.2	56.0	280.0	0.0
11.4	11.4	57.0	285.0	0.0
11.6	11.6	58.0	290.0	0.0
11.8	11.8	59.0	295.0	0.0
12.0	12.0	60.0	300.0	0.0
12.2	12.2	61.0	305.0	0.0
12.4	12.4	62.0	310.0	0.0
12.6	12.6	63.0	315.0	0.0
12.8	12.8	64.0	320.0	0.0
13.0	13.0	65.0	325.0	0.0
13.2	13.2	66.0	330.0	0.0
13.4	13.4	67.0	335.0	0.0
13.6	13.6	68.0	340.0	0.0
13.8	13.8	69.0	345.0	0.0
14.0	14.0	70.0	350.0	0.0
14.2	14.2	71.0	355.0	0.0
14.4	14.4	72.0	360.0	0.0
14.6	14.6	73.0	365.0	0.0
14.8	14.8	74.0	370.0	0.0
15.0	15.0	75.0	375.0	0.0
15.2	15.2	76.0	380.0	0.0
15.4	15.4	77.0	385.0	0.0
15.6	15.6	78.0	390.0	0.0
15.8	15.8	79.0	395.0	0.0
16.0	16.0	80.0	400.0	0.0
16.2	16.2	81.0	405.0	0.0
16.4	16.4	82.0	410.0	0.0
16.6	16.6	83.0	415.0	0.0
16.8	16.8	84.0	420.0	0.0
17.0	17.0	85.0	425.0	0.0
17.2	17.2	86.0	430.0	0.0
17.4	17.4	87.0	435.0	0.0
17.6	17.6	88.0	440.0	0.0
17.8	17.8	89.0	445.0	0.0
18.0	18.0	90.0	450.0	0.0
18.2	18.2	91.0	455.0	0.0
18.4	18.4	92.0	460.0	0.0
18.6	18.6	93.0	465.0	0.0
18.8	18.8	94.0	470.0	0.0
19.0	19.0	95.0	475.0	0.0
19.2	19.2	96.0	480.0	0.0
19.4	19.4	97.0	485.0	0.0
19.6	19.6	98.0	490.0	0.0
19.8	19.8	99.0	495.0	0.0
20.0	20.0	100.0	500.0	0.0

RESULTS OF DISTRIBUTED TEMPERATURE AFTER 24 ITERATIONS AND TIME OF 96-00 HOURS AND HEAT INPUT QP = 0.00 AT THE DAY OF 4

卷之三

ACKNOWLEDGEMENT

I wish to extend my sincere thanks to Professor Robert L. Gorton for all his efforts in the organization of this paper and for his thoughts on writing it. His knowledge of computer techniques was invaluable as was his encouragement; and his patience in listening is appreciated.

I wish also to thank Dr.'s Gary Johnson and Hugh Walker for their computer programming ideas and their discussions of solving computer program problems. I also appreciate the thoughts and suggestions of Dr.'s Herbert Ball, Terry Beck, and Byron Jones on this project.

Special thanks to my wife for her support and companionship, and her time and efforts in typing this thesis as well as for her English grammar discussions.

Thanks also to all the friends who contributed their ideas and suggestions to this paper.

This work was supported primarily by the Kansas Electric Utilities Research Program (KEURP Project KRD79), Mr. Pete Loux, Director, and Mr. Alan Kettle, Project Engineer. I am grateful for this support and for the partial support of the KSU Engineering Experiment Station.

VITA

Trung Q. Hoang

Candidate for the degree of
Master of Science

Thesis: A MATHEMATICAL MODEL FOR TEMPERATURE AND HEAT LOSS CHARACTERISTICS OF UNDERFLOOR ELECTRIC RESISTANCE HEATING AND STORAGE SYSTEM

Major Field: Mechanical Engineering

Biographical:

Personal Data: Born in Hanoi, Vietnam, July 24, 1950, the son of Mr. Bao T. Hoang and Mrs. Tru T. Nguyen.

Education: Graduated from Hung Dao High School, Saigon in July 1970; received Bachelor of Science degree from Kansas State University with a major in Mechanical Engineering in May 1983; completed the requirements for the Master of Science degree in June 1985.

Societies: American Society of Heating and Air Conditioning Engineers; National Society of Professional Engineers.

A MATHEMATICAL MODEL FOR TEMPERATURE AND HEAT LOSS CHARACTERISTICS
OF UNDERFLOOR ELECTRICAL RESISTANCE HEATING AND STORAGE SYSTEM

by

TRUNG QUANG HOANG

B.S., Kansas State University, 1983

AN ABSTRACT OF A MASTER'S THESIS

submitted in partial fulfillment of the

requirements for the degree

MASTER OF SCIENCE

Department of Mechanical Engineering

KANSAS STATE UNIVERSITY
Manhattan, Kansas

1985

ABSTRACT

Underslab thermal heating and storage systems have been built for one-story buildings because of lower electricity rates which may be available for off-peak use. Very few studies have been done on determination of the heat flow and temperature behaviors of buildings using such systems. An investigation of the heat flow and temperature characteristics of an existing building were initiated with a computer model and then compared to operation of an actual system. A mathematical model was developed for a transient, two-dimensional, and finite difference heat transfer system to represent storage bed, building, and surrounding earth, both adjacent to and under the building floor. This model was used to determine the influence of numerous parameters which affect the building heat flows and temperature patterns.

The parameters designated in the study are soil properties, building thermal transmittance, edge insulation thickness, heat input intensity, time-operating schedule, and climatic conditions. These parameters were studied for their effect on an on-grade building, and for a below-grade building with an embankment.

The results of parametric study shows the advantage -- building temperatures differed only a few degrees ($^{\circ}\text{F}$) from floor to ceiling temperatures. Thus, level of human comfort is easier to maintain than with a conventional heating system. Also, the system may cost less than a conventional heating system for energy use if a low rate of "off" peak electricity is offered.

ABSTRACT

(Continued)

However, a sophisticated control system is essential to anticipate heating load and provide the proper economics.

The results derived here from the parametric study can be used as a tool for designing a system as well as for an operation guide to control the system efficiently.